

FINAL REPORT

**NEW METHODOLOGIES FOR MEASURING AND MONITORING
HYDROGEN FOR SAFETY IN ADVANCED HIGH STRENGTH
LINE PIPE STEEL**

**Development of a Non-Destructive Non-Contact Electromagnetic
Sensor for Hydrogen Content Determination in Coated Line Pipe
Steel**

Contract Number: **1435-01-04-36637**

CSM Project Number.: 4-42482

CSM Report Number.: MT-CWJCR-007-002

Submitted to:

MINERAL MANAGEMENT SERVICES

Attn: **MICHAEL ELSE**

US DEPARTMENT OF THE INTERIOR
Technology Assessment & Research Branch
381 Elden St., MS 4700
Herndon, VA 20170-4817

Attn: **KIMBERLY LUKE**

U.S. DEPARTMENT OF THE INTERIOR
Mineral Management Service
381 Elden St., MS 2500
Herndon, VA 20170-4817

Attn: **ROBERT SMITH**

US DEPARTMENT OF TRANSPORTATION
Office of Pipeline Safety
400 7th St., SW
Washington, D.C. 20590

Submitted by:

David L. Olson
Brajendra Mishra
Angelique N. Lasseigne

February 28, 2007

COLORADO SCHOOL OF MINES

Abstract

The assessment of the hydrogen content in pipeline steel is an essential requirement to monitor loss of integrity with time and prevent failures. With the use of pipeline steels of increasing strength, the threshold of hydrogen concentration for hydrogen cracking is significantly being reduced. Cathodic protection and corrosion processes both contribute to accumulation of hydrogen as a function of time. Continued accumulation of hydrogen with time will eventually meet the cracking criteria.

New and unique methodologies based on electronic property measurements offer the pipeline industry non-destructive tools to achieve this hydrogen content assessment in-situ and in real-time. The use of thermoelectric power, a surface contact non-destructive measurement can assess hydrogen in pipeline steels while the pipe is exposed without coating. A non-contact through-coating technique has also been developed to assess hydrogen through the pipe coating. The induced current low-frequency impedance technique is a cost-effective practice to monitor the hydrogen accumulation in high-strength steel pipelines. This report describes the scientific basis and engineering practice to utilize both of these advanced electronic property measurement techniques. These advanced techniques have been successfully demonstrated to assess hydrogen content in linepipe steel. The practice of determining the equivalent microstructure or steel properties from which standards for hydrogen determination can be produced is also described.

Table of Contents

Table of Contents.....	3
1. Objective.....	4
2. Introduction.....	4
3. Background and Justification for Performing Research.....	5
3.1. Role of Hydrogen in Pipelines.....	7
3.1.1. Hydrogen Solubility.....	7
3.1.1.1. Hydrogen Damage.....	11
3.2. Non-Destructive Tools for Hydrogen Sensor Development.....	13
3.2.1. Electromagnetic Non-Contact Hydrogen Sensor.....	14
3.2.2. Electromagnetic Theory.....	15
3.2.2.1. <i>Induced Current Resistivity (Eddy Currents) Analysis</i>	15
4. Experimental Plan.....	22
4.1. Specimen Preparation for Hydrogen Measurements.....	22
4.2. Electromagnetic Probe Development for a Hydrogen Sensor.....	26
4.3. Electromagnetic Sensor Development for Temperature and Microstructure Corrections.....	30
4.3.1. Specimen Preparation for Temperature Measurements.....	31
4.3.2. Specimen Preparation for Microstructure Measurements.....	31
4.4. Low Frequency Impedance Through a Coating.....	32
5. Experimental Results.....	32
5.1. Electromagnetic Hydrogen Sensor.....	32
5.2. Electromagnetic Coil Development.....	36
5.3. Electromagnetic Temperature Measurements.....	39
5.4. Electromagnetic Microstructure Measurements.....	39
5.5. Low Frequency Impedance Measurements Through a Coating...	42
6. Analysis of Results.....	42
6.1. Electromagnetic Hydrogen Sensor.....	42
6.2. Electromagnetic Coil Development.....	46
6.3. Electromagnetic Temperature Sensor.....	47
6.4. Electromagnetic Microstructure Sensor.....	47
6.5. Low Frequency Impedance Measurements Through a Coating...	48
7. Portable Electromagnetic Probe Development.....	48
8. Application of In-field Impedance Analyzer.....	49
9. Conclusions.....	50
10. Future Work and Recommendation.....	51
11. References.....	51

1. Objective

The objective of this study was development of a non-destructive, non-contact tool to measure diffusible hydrogen in coated line pipe steel.

2. Introduction

With the rapid introduction of high strength linepipe steels (in excess of 70 ksi yield strength) for operation and use at higher pressures and reduced wall thicknesses, the need for new approaches for hydrogen management must be addressed. With increasing steel strength there is a reduction in the allowable diffusible hydrogen content to avoid hydrogen assisted cracking. Hydrogen-assisted cracking and hydrogen embrittlement are common terms used to describe sub-critical cracking due to hydrogen in metals. Hydrogen damage refers to the action of hydrogen reducing the physical and mechanical properties of a material to a degree that renders it unattractive, fallacious, or dangerous (Beachem, 1977).

Hydrogen can be introduced into the linepipe steel in numerous ways; for example, through welding procedures, cathodic protection, corrosion reactions with the environment, and interactions with the contained media in the pipes. Research efforts in hydrogen damage are seriously hampered because the equipment available only measures the total effects of very large numbers of hydrogen molecules, ions, or protons, as they act on a specimen or service component [Beachem, 1977]. Advanced research has led to the improvement and development of hydrogen determination tools, which has led to numerous non-destructive methods capable of measuring hydrogen content in steel and weldments. These techniques are, however, all contact techniques and, since pipelines are coated, it is necessary to develop a non-contact technique that can perform measurements through the pipeline coating.

This project has advanced the available technology to measure and monitor the diffusible hydrogen content and increased our understanding of hydrogen management. Through the use of complimenting electromagnetic techniques, a new non-destructive, non-contact tool has been developed for in-situ determination of diffusible hydrogen content in coated linepipe steel. The electromagnetic techniques allow for a means of measurement of hydrogen accumulation without damaging the linepipe coating. These tests establish a threshold electromagnetic property value for a given steel grade that enables measurement of the threshold when sufficient hydrogen has been absorbed to lead to a reduction in the integrity of the pipeline.

3. Background and Justification for Performing Research

The ever-increasing demand for energy worldwide requires the construction of high-pressure gas transmission lines with the greatest possible transport efficiency while reducing the cost of pipeline construction and operation. In North America alone, the total length of high-pressure gas transmission pipelines is greater than 300,000 miles. In large diameter pipelines (OD: 48 to 56 inches (1212 - 1422 mm)), outage costs may be as high as one million dollars per day. In 2004, there were over 36 corrosion-caused pipeline ruptures with an average cost of over 13 million dollars.

New pipeline steels have been under development for over 40 years to provide better transport efficiency through larger diameter pipelines with a reduction in wall thickness, such as X80 linepipe steel. X80 linepipe steel is currently available in the market. X80 is chosen and designed for linepipe steel because it has high strength with good weldability and toughness. X80 is not dependent upon the chemical composition, but depends on the strength of 80 ksi. X80 was first used in 1985 on a 3.5 km line on a trial basis. Germany then reproduced the X80 steel for use in longer pipelines across Germany. Hydrogen cracking is a major problem associated with in-service pipelines, especially high strength steel pipelines.

In pipelines, there are numerous sources responsible for the production of hydrogen, some of which include welding procedures, cathodic protection, and corrosion reactions with the environment and with the contained media in the pipes. The most common source of hydrogen is from cathodic reduction of hydrogen and water during cathodic protection. The presence of hydrogen can lead to detrimental results in these high-pressure steel pipelines. Hydrogen damage reduces the physical and mechanical properties of a material to a degree that renders it unattractive, fallacious, or dangerous (Beachem, 1977). Because it is impossible to remove hydrogen from the system (pipeline), the hydrogen must be monitored in the system.

"The future of pipeline integrity is in the management and interaction of collected survey data" [Author unknown]. This statement should be taken very seriously because the only way to monitor a pipeline that cannot physically be inspected is through surveying data. There are many intelligent non-destructive tools offered on the market, which are used industrially for crack, surface, and corrosion inspections. Some of these non-destructive tools include eddy currents, magnetic flux leakage, ultrasonic, magnetic Barkhausen noise, etc. [Griffith et al, 1997], [Mandal et al, 1999], [Crouch and Beuker, 2004]. These non-destructive tools are necessary to guarantee pipe integrity, however these tools do not assess diffusible hydrogen until significant cracking occurs. New tools need to be developed to monitor the diffusible hydrogen content before significant defects arise.

There are many methods and sensors available for diffusible hydrogen measurements, however a non-destructive technique is necessary for in-service hydrogen content measurements. Thermoelectric power (Seebeck effect) has been experimentally and thermodynamically proven to non-destructively measure diffusible hydrogen content in steel. The downfall to thermoelectric power for assessment of hydrogen in pipelines is that it is a surface contact measurement, which means measurements cannot be made through a coating. With this in mind, the focus of this research is to develop a new non-destructive, non-contact probe that can measure diffusible hydrogen content in coated linepipe steel.

The "ideal" NDE tool for such testing must be able to quickly determine the quantity, distribution, and the transport relationship of hydrogen to microstructural constituents and possible related failure mechanisms. Diffusible hydrogen is transient, *i.e.* the concentration and distribution are continually changing with time. Hydrogen migrates to dislocations, second phase particles, voids, etc. in the pipeline steel material, and these defects influence both the distribution and the mobility of hydrogen. Therefore, it is insufficient to simply measure the total hydrogen content in a specimen. Instead, we must develop new tools that are sensitive to degree of interaction of the hydrogen once it enters the material.

The oil and gas industry currently utilizes a pipeline cleaning technique driven by product flow called pigging. A pig is a cleaning device that is pushed through the pipeline to remove deposits and water that could cause corrosion, but as the pig removes the residue, it is sequentially eliminating any films or deposits that may also be protecting the surface from corrosion. With this limitation in mind, "smart pigs" were designed, which includes cleaning and deposition removal as well as magnetic flux leakage (MFL) unit that can monitor the pipeline for cracks and defects. In MFL, a magnetic flux is generated in the pipeline and if there is a defect or a crack, the magnetic flux will leak in that area. The MFL unit is a precautionary tool to find potential problems.

The "smart pig" is an important factor in this research because recent experiments performed at the Colorado School of Mines have found that magnetic flux in pipeline steel increases the solubility of hydrogen by a factor of three. These experimental findings play an important role in the integrity of pipelines, thus increasing the need for a tool to monitor the diffusible hydrogen content in pipelines.

The following sections will discuss the role of hydrogen in pipelines and the consequences of hydrogen in pipelines. A discussion is then given on the development of a new non-contact, non-destructive method for assessment of diffusible hydrogen in coated linepipe steel.

3.1. Role of Hydrogen in Pipelines

Hydrogen is the smallest element in the periodic table, so that when hydrogen enters the iron lattice it occupies interstitial sites. Hydrogen migrates to dislocations, second phase particles, voids, etc. in the material, thus influencing the distribution and mobility of hydrogen. Hydrogen is transient, the concentration and distribution is continually changing with time.

Due to the abundance of hydrogen sources in pipelines, it is important to quantify the amount and form of hydrogen present in the steel because there is a distinction between total, residual, and diffusible hydrogen. Diffusible hydrogen is considered to be mobile at lower temperatures (<100°C), whereas the remaining residual hydrogen is trapped in the metal at microstructural discontinuities or by the formation of hydrides with alloying elements. Total hydrogen is the combination of the two fractions. Each form of hydrogen exhibits different properties. For example, diffusible hydrogen increases dislocation motion, whereas dislocation motion would be temporarily hindered by a formed hydride because the dislocation will have to cut or bow around it (dependent upon the shear stress). It is also well established that the formation and fracture of brittle hydrides promote hydrogen-assisted cracking.

The formation of second phase particles is related to the atomic nature of hydrogen. Elements on the periodic table to the left of manganese are electron acceptors, having a negative heat of mixing, resulting in the formation of hydrides. The elements on the periodic table to the right of manganese are electron donors with a positive heat of mixing meaning that hydrogen stays in solution.

The solubility and diffusivity of hydrogen differ greatly between iron phases. The solubility of hydrogen in austenite is very large, while being very small in ferrite. The diffusivity of hydrogen in austenite is very slow, but much quicker in ferrite, thus meaning that austenite is a diffusion barrier for hydrogen transport, while ferrite facilitates hydrogen transport.

3.1.1. Hydrogen Solubility

When hydrogen enters the metal lattice it dissociates into a proton and an electron. The proton occupies the interstitial site in ferrous alloys and the electron is donated to the host metal electronic d-band. The proton is very small when compared to the size of the interstitial site. The positive charge of the proton must be screened to maintain the electrical neutrality [Pepperhoff and Acet, 2001]. The electrical neutrality is preserved by the formation of an atomic sized electron cloud, however this process is not perfect so that repulsive forces occur between the proton and the neighboring positively charged metal nuclei. These

repulsive forces result in a local expansion and lattice distortion. Figure 1 shows the change in volume of the unit cell with increasing hydrogen concentration due to the repulsive forces from the electron cloud. Hydrogen does not only cause large lattice distortion, but it also contributes to the chemical potential of the electron in the metal. Figure 2 shows the change in the chemical potential in zirconium nickel alloys due to the addition of hydrogen atoms. The chemical potential is the upper most filled electron band, otherwise known as the Fermi energy. The solubility of hydrogen in the metal lattice is affected by the electronic filling of the host metal electronic conduction bands by other metallic solutes because there must be space for hydrogen to donate its electron.

Hydrogen traps [Maroef *et al.*, 2002] also play a role in the solubility of hydrogen because it literally traps the hydrogen atoms, no longer allowing the hydrogen to diffuse through the metal lattice. At lower temperatures, hydrogen prefers to occupy tetrahedral sites and at higher temperatures, hydrogen prefers the occupation of octahedral sites.

Sieverts' law holds true for hydrogen because hydrogen gas molecules become dissociated into atoms while being dissolved into metals in the region where hydrogen can be regarded as an ideal gas. At higher pressures and temperatures, the chemical potential and solubility of hydrogen deviates from the ideal gas behavior, thus Sieverts' law no longer applies. The chemical potential of hydrogen gas increases dramatically at even higher pressures resulting in a great solubility enhancement [Fukai, 1993]. As with nitrogen, there are many factors affecting the solubility and diffusivity of hydrogen in metals.

Thomas Graham coined the term "occlusive capacity" defined as the concentration of hydrogen within a compact metal when it has established a steady state of exchange with hydrogen gas of certain temperature and pressure [Smith, 1948]. The occlusive capacity is the solubility dependent on the degree of strain or plastic deformation [Beck *et al.*, 1965]. The occlusive capacity is important because hydrogen tends to accumulate in regions of high stress (stress-assisted hydrogen diffusion). There are many regions of high stress in pipelines. Some examples high stress regions include: (1) heat-affected zones (2) grain boundaries, (3) voids, and (4) crack tips. The most common types of cracks occurring in pipelines are hydrogen induced cracks, fatigue cracks, stress corrosion cracks, and cracks in the weld HAZ. The occlusive capacity describes the true solubility of hydrogen in the pipeline due to stress.

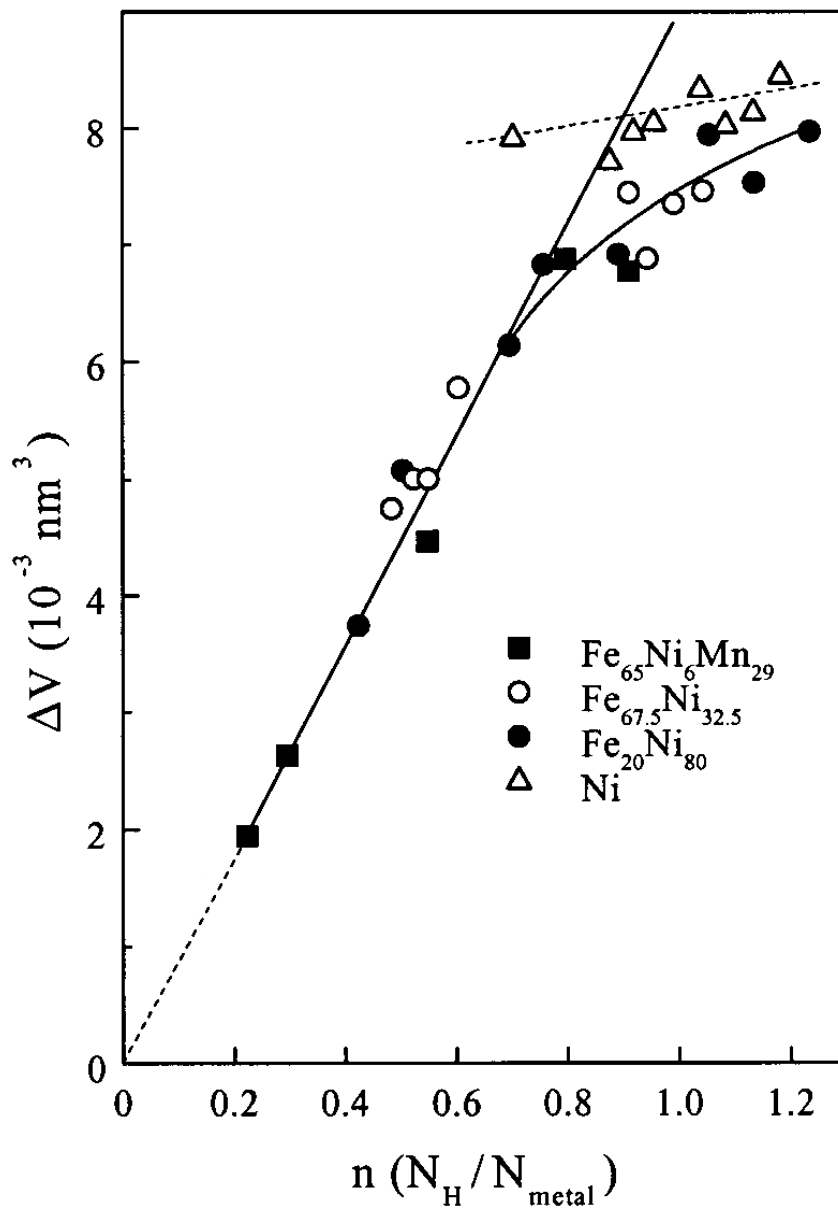


Figure 1: Increase in volume in the unit cell with increasing hydrogen concentrations at $T=38^\circ\text{K}$ and atmospheric pressure [Pepperhoff and Acet, 2001].

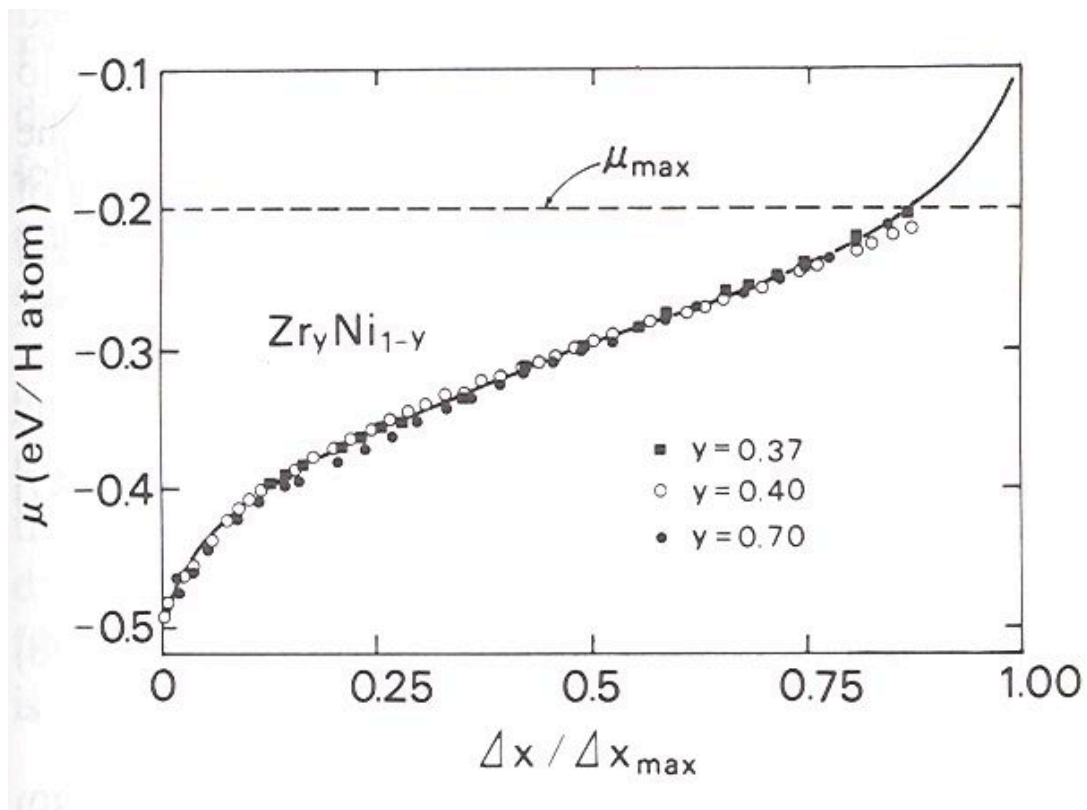


Figure 2: Chemical potential of hydrogen in amorphous Zr_yNi_{1-y} alloys plotted against normalized variations in hydrogen content. The upper limit corresponds to the standard state of hydrogen gas at 295°K and 1 atm [Harris *et al.*, 1987].

Figure 3 shows the importance of the occlusive capacity because variations in hydrogen content play a vital role on the stress state for crack growth during hydrogen assisting cracking and stress corrosion cracking. The concentration of hydrogen at a crack tip will change the mode of hydrogen cracking at a particular stress intensity factor [Beachem, 1972]. The curved dashed lines indicate critical combinations of stress intensity factor and hydrogen content for the cause of crack growth by the three fracture modes. The existence and position of each of the curves are microstructure dependent, so this graph does not hold true for all materials. Below the lowest curve, no hydrogen cracking is expected. Each of the curves are drawn to meet at the critical stress intensity factor because quench and tempered steels tend to exhibit one or all of these fracture modes when failure occurs in the absence of induced hydrogen [Beachem, 1972].

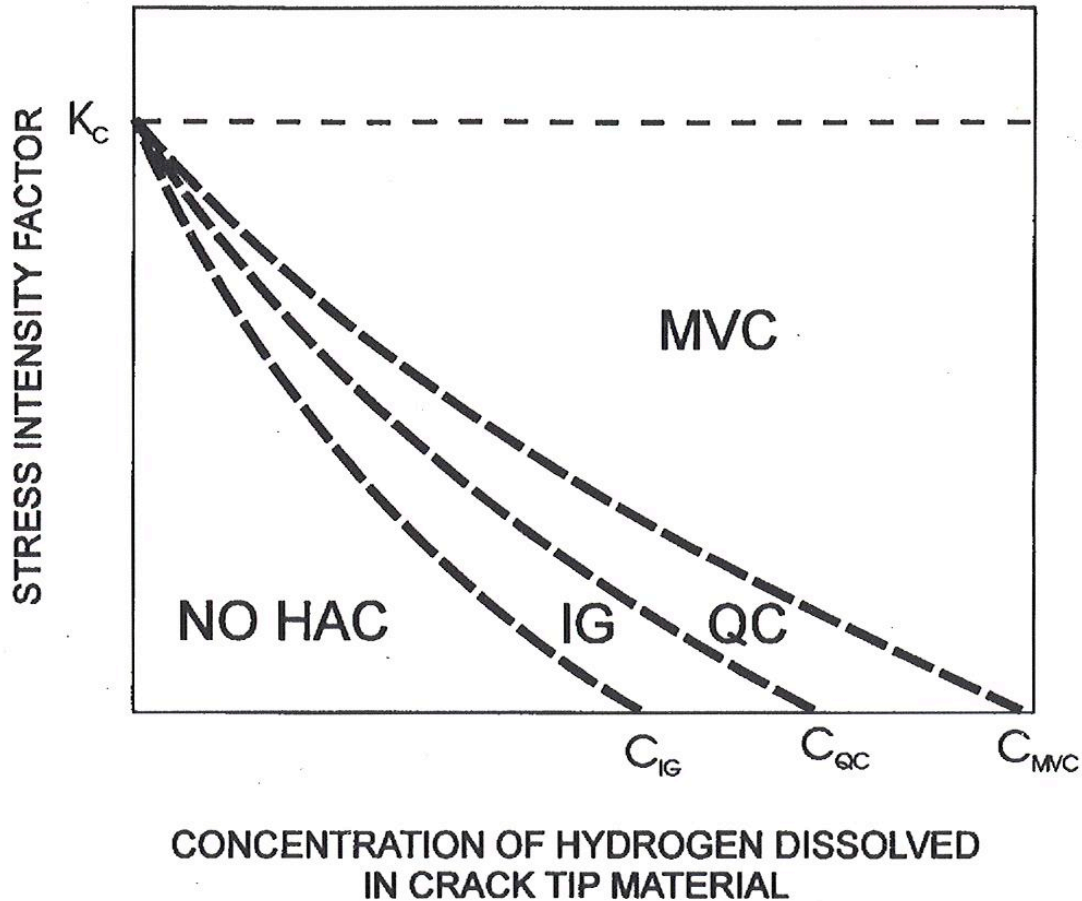


Figure 3: Suggested interrelationships between stress intensity factor as a function of dissolved hydrogen concentration in microscopically volumes of crack tip material showing the changes in hydrogen assisted cracking failure modes. (IG: Intergranular, QC: quasi-cleavage, MVC: micro-void coalescence) Beachem 1972.

3.1.1.1. Hydrogen Damage

Hydrogen damage has been divided into three different forms. One form of damage results in internal pores, cracks or other flaws arising from either the entrapment of hydrogen bubbles during solidification of the melt or diffusion of hydrogen through the metal lattice to cause flaws. At higher temperatures, hydrogen reacts predictably to alter chemical compositions to form collecting pockets of gaseous molecules that cannot escape by diffusion and remains trapped. The second form of damage results when formed hydrides assume specific lattice positions within the metal, thus lowering the mechanical properties and the toughness of the metal. The third form of hydrogen damage results despite the absence of a known chemical reaction or hydride formation; nevertheless the hydrogen causes crack formation and growth, particularly in the

presence of sustained stress. This form of damage is called hydrogen-assisted cracking (otherwise known as hydrogen embrittlement) [Buzzard and Cleaves, 1951], [Johnson, 1873-1875], [Troiano *et al.*, 1974], [Beachem, 1977]. This third type of damage has been related to localized microplasticity in the region of the triaxial stress at the crack tip.

The following conditions must be met for the occurrence of hydrogen assisted cracking: (1) sufficient atomic hydrogen in the material, (2) tensile stress, (3) susceptible material, (4) temperature range that supports very localized hydrogen transport (-50 to 150°C in steel). When these conditions are met, in non-hydride forming elements, there are three mechanisms of hydrogen embrittlement worthy of consideration [Darken and Smith, 1949], [Beck *et al.*, 1966] [Lynch, 1991]. These mechanisms include: (1) hydrogen-enhanced localized plasticity, (2) hydrogen-enhanced de-cohesion, and (3) adsorption-induced dislocation emission. These mechanisms have been proposed for embrittlement in external (H₂, H₂S, H₂O) and internal (introduced into steel during welding, plating, etc) hydrogen environments [Lynch, 2001]. It should be recognized that the cracking mechanisms could be similar, however the rate controlling processes are very different.

Hydrogen-Enhanced Localized Plasticity (HELP)

Hydrogen-enhanced localized plasticity is based on the presence of solute hydrogen ahead of cracks, specifically in hydrogen atmospheres around both mobile dislocations and obstacles to dislocations [Paskin *et al.*, 1983, 1984] [Thomson, *et al.*, 1986], [Daw and Baskes, 1984], [Lynch, 1999], [Beachem, 1972]. It has been suggested that the hydrogen atmospheres distort when mobile dislocations approach obstacles, meaning that the repulsion by obstacles is decreased. Since hydrogen accumulation is localized near crack-tips, deformation is localized and facilitated near crack-tips, resulting in an overall lower strain for fracture [Lynch, 1999, 2001].

Hydrogen-Enhanced Decohesion (HEDE)

Hydrogen-enhanced decohesion is the weakening of iron-iron intermetallic bonds at or near crack tips due to high localized hydrogen concentrations in the lattice resulting in tensile separation of the atoms [Oriani, 1972, 1977], [Troiano, 1960]. The weakening of bonds may be the result of a decrease in the electronic charge density between metal-metal atoms due to the existence of hydrogen in the crystal lattice in interstitial sites [Lynch, 2001]. For hydrogen-enhanced decohesion, fracture surfaces should appear basically featureless with a few cleavage steps and tear ridges separating de-cohered regions [Lynch, 1999].

Adsorption Induced Localized Slip (AIDE)

Adsorption induced localized slip is based on hydrogen-induced weakening of interatomic bonds, but with crack growth occurring by

localized slip [Birnbaum, 1994], [Lynch, 1999]. It has been proposed that adsorbed hydrogen weakens substrate interatomic bonds and thereby facilitates the emission of dislocations from the crack tips. There is also substantial dislocation emission ahead of the crack tip, resulting in the formation of voids around particles or at slip band intersections. This behavior means that crack propagation occurs due to dislocation emission from crack tips also with a contribution from the void formation ahead of the crack tip [Birnbaum, 1994], [Lynch, 1999, 2001].

A combination of these three mechanisms occurs in most cases. Figure 4 schematically illustrates the HEDE, HEDE, and AIDE. The most dominant mechanism will be dependent upon variables such as strength, microstructure, slip-mode, stress intensity factor, and temperature, thus affecting the fracture path and appearance [Lynch, 2001].

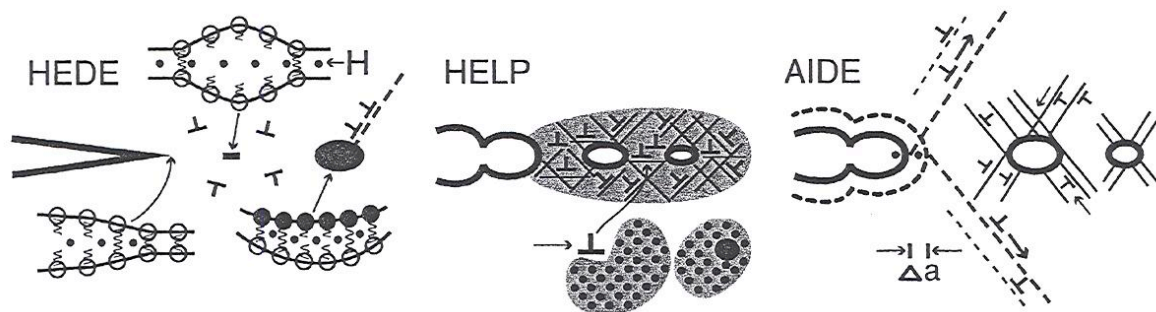


Figure 4: Schematic diagrams illustrating HEDE, HELP, AIDE mechanisms of hydrogen-assisted cracking [Lynch, 2001].

3.2. *Non-Destructive Tools for Hydrogen Sensor Development*

Multiple techniques have been developed for use as hydrogen sensors. Some of these techniques include volumetric displacement, gas chromatography, laser ablation with mass spectrometry, laser ablation with gas chromatography, and opto-electronic diffusible hydrogen sensors.

Volumetric displacement is the standard AWS method for measuring hydrogen in weld specimens. In this method a sample is placed into a eudiometer and allowed to evolve hydrogen at temperatures varying from 45 to 150°C [AWS, 1993]. The evolved gas displaces the mercury in the top of the column and the amount of displacement is measured as a function of volume. The results are reported as a function of milliliter of hydrogen per 100 grams of deposited weld metal [AWS, 1993]. Due to the increased health concerns of using mercury displacement testing, gas chromatography has become another very popular method.

In gas chromatography, hydrogen specimens are placed in sealed containers and baked to release the hydrogen. The evolved gas is transferred to a gas chromatograph and then separated with a packed molecular sieve column to be analyzed using a thermal conductivity detector. The gas chromatograph gives comparable results to mercury testing [AWS, 1993], [Quintana, 1988].

Laser ablation methods use laser energy to release diffusible hydrogen from the surface to allow for the determination of hydrogen levels in particular areas on weld surfaces. Laser energy releases very small amounts of hydrogen, thus requiring very sensitive detection methods such as mass spectrometry [Smith *et al.*, 1999, 2001]. The presence of organic material on the surface poses problems due to decomposition and hydrogen formation from the contaminants in the laser plasma.

The opto-electronic diffusible hydrogen sensor utilizes the optoelectronic properties of hydrogen sensitive material such as tungsten oxide to generate analytical signals [Smith *et al.*, 1997]. When hydrogen is absorbed on the surface it reacts to form an ion insertion compound. The optical properties of the compound are altered and can be detected visually or spectroscopically. The opto-electronic diffusible hydrogen sensor takes approximately one hour and can be utilized on actual welds as opposed to laboratory specimens.

3.2.1. Electromagnetic Non-Contact Hydrogen Sensor

Advanced research has led to the improvement and development of hydrogen determination tools discussed above, which has led to numerous non-destructive methods capable of measuring hydrogen content in steel and weldments. These techniques are, however, all contact techniques and, since pipelines are coated, it is necessary to develop a non-contact technique that can perform measurements through the pipeline coating. When properly calibrated and standardized, electromagnetic techniques allow for non-contact, non-destructive measurements of interstitial contents.

Most non-destructive electromagnetic tools currently utilized in industry (ultrasonic, magnetic flux leakage, etc.) are used for determination of existing cracks, flaws, defects, etc., in other words, characterization after the fact. The development of a non-destructive diffusible hydrogen meter will allow for property prediction before significant defects or cracks occur. The non-destructive diffusible hydrogen meter can beneficially be used during production and in-service.

There are many variables associated with pipelines, such as temperature, pressure, steel, coatings, etc. This research will apply a combination of different complimenting, non-contact electromagnetic methods to determine the diffusible hydrogen content in coated linepipe

steel. The methods investigated in this research will include eddy current analysis for impedance measurements, magnetic Barkhausen noise analysis (MBN), and electromagnetic acoustic transducer analysis (EMAT). The MBN and EMAT techniques are necessary to correct for the temperature, microstructure, and composition to allow proper standardization for the eddy current assessment of the hydrogen content. Each of these non-destructive techniques are currently utilized for pipeline inspection, however they are used individually for crack, defect, and corrosion monitoring. These methods will be used together to eliminate any additional variables to rapidly generate a quantitative hydrogen content associated with the coated linepipe steel.

3.2.2. Electromagnetic Theory

Eddy currents, magnetic Barkhausen noise, and electromagnetic acoustic transducers are based on Faraday's law. Faraday's law states that, "a changing magnetic field induces an electric field." Faraday's law really distinguishes between two types of electric fields: (1) those attributed to electric charges and (2) those associated with changing magnetic fields. The curl of an electrostatic field is given by the differential form of Faraday's law is:

$$\nabla \times E = -\frac{\partial B}{\partial t} \quad [1]$$

where ∇ is the del operator, E is the electrostatic field, B is the magnetic flux density, and t is time.

3.2.2.1. Induced Current Resistivity (Eddy Currents) Analysis

Eddy Current analysis is a technique generally utilized to find near surface defects in alloy parts, normally in non-ferrous alloys. The ferromagnetic behavior of steel causes a significant change in the steel's impedance, which hinders the determination of cracks, but should serve as an excellent indicator for diffusible hydrogen content in the near surface region of the steel. Since diffusible hydrogen donates its electron to the d-band of steel, which is the same band that contributes to the ferromagnetic behavior, the induced current in the steel will experience the change in resistivity due to the hydrogen and will cause perturbation in the eddy current signal. Eddy currents units have been designed and experimentally proven for flaw, cracks, and thickness examination of large diameter pipelines through coatings and insulation [Griffith *et al.*, 1997].

In eddy current testing, a high or low frequency electromagnetic (EM) field is generated in a conductor by an alternating current. When placed in close proximity of a material, the generated EM field induces currents (eddy currents) within the inspected material. In response, the eddy currents induced in the inspected material generates a magnetic field. The EM fields from the induction coil and the inspected material must be detected either by electromagnetic induction in a coil, by a system of coils, or by sensors such as the Hall element. In many cases the same coil is used both to excite the eddy currents, and also to detect their fields.

A significant advantage of the eddy current technique is that it can be performed at a stand off distance and through the pipeline coating. The first step in using the eddy current testing practice is to select all of the controllable parameters in such a way as to optimally detect the desired material parameter. For the proposed hydrogen sensing investigation the initial part of the effort will be to determine the optimum set of controllable parameters.

The relationship between the current flowing through a coil and the resulting magnetic field strength, H , was discussed. The magnetic field strength produces a magnetic flux density, B , and a flux, ϕ , which is defined as the integral of the magnetic flux density over a particular surface given as:

$$\phi = \int B \cdot nda \quad [2]$$

During induced current resistivity (eddy current) measurements, the coil is held close to the sample, so that the flux created by the coil affects the sample. The coil parameters and primary excitation current are a function of the flux. The oscillating nature of the flux induces eddy currents in the sample beneath the coil. The eddy currents produce their own magnetic field, which opposes the field, which produced them (Lenz's law) [Bray and Stanley, 1997]. The coil then senses an equilibrium flux, which is the difference between the induced primary flux and the secondary flux due to the sample [Bray and Stanley, 1997].

When AC current is applied, the coil possesses both resistance and reactance. Along with resistance, there is a changing flux in the coil, which exhibits inductance [Bray and Stanley, 1997]. The coil's inductance is the flux linkage change per unit current and is given as:

$$L = d(N\phi)/dI \quad [3]$$

where N is the number of turns in the coil and I is the current. The inductive reactance occurs when a coil is excited at an angular frequency, ω , creating another form of resistance due to a generated back electromotive force caused by the changing flux linkage within [Bray and Stanley, 1997]. The magnitude of the inductive reactance, X_L , is given as:

$$X_L = \omega L = 2\pi f L \quad [4]$$

where f is the frequency, which would be zero in a direct current. The phase of the current through the coil is common to both components, so that if the phase is drawn electrically as shown in Figure 5 then the voltage across the resistive and inductive parts are IR and $I\omega L$ as shown in Figure 6 [Bray and Stanley, 1997]. Figure 6 shows the right triangle created by the resistive and inductive parts so that the total circuit voltage, V , becomes:

$$V = I ((\omega L)^2 + R^2)^{1/2} \quad [5]$$

Then using Ohm's law, where $V = IZ$, the total impedance exhibited in the coil is given as:

$$Z = ((\omega L)^2 + R^2)^{1/2} \quad [6]$$

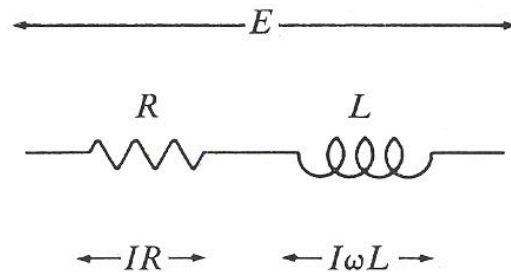


Figure 5: Generalized coil [Bray and Stanley, 1997].

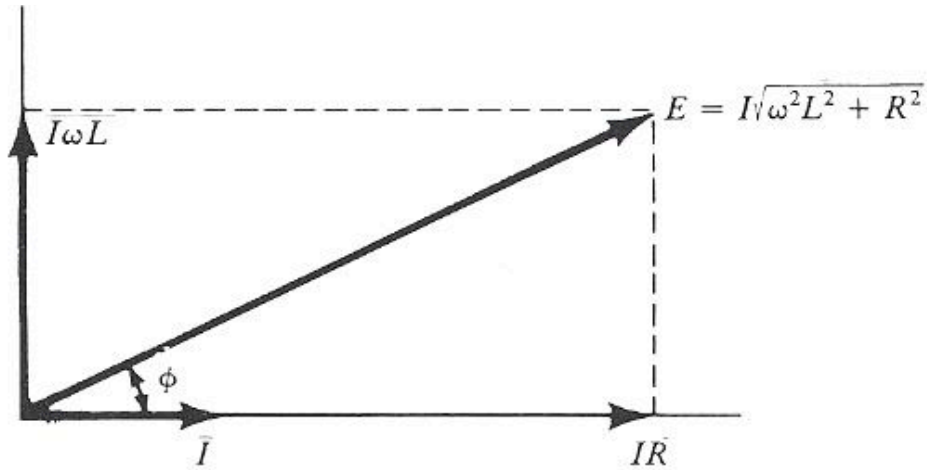


Figure 6: Vector relations between resistance and inductive parts for a coil [Bray and Stanley, 1997].

The total impedance of the coil will also have an often-negligible term called the capacitance [Bray and Stanley, 1997]. The capacitance reactance of the coil, X_c is given by:

$$X_c = 1/(\omega C) = 1/(2\pi f C) \quad [7]$$

where C is the capacitance in farads. Capacitance reactance may play a role during the use of coil probes attached to the eddy current instrument by very long wires [Bray and Stanley, 1997]. When a circuit contains both inductance and reactance, the total impedance of the coil becomes:

$$Z = ((\omega L - 1/\omega C)^2 + R^2)^{1/2} \quad [8]$$

and the phase angle, ϕ , between the current in and voltage across the circuit is given by:

$$\tan \phi = (\omega L - 1/\omega C)/R \quad [9]$$

It can be seen that the possibility arises that, if $\omega L = 1/\omega C$, and C and L are equal to zero then the impedance becomes only a function of the resistance, and the phase angle becomes zero degrees [Bray and Stanley,

1997]. This condition is known as resonance, and many circuits are designed to operate at or near such a condition.

The eddy current density, and thus the strength of the response from a flaw, is greatest on the surface of the metal being tested and the strength declines with depth [Bray and Stanley, 1997]. It is mathematically possible to define the "standard depth of penetration" where the eddy current is 1/e (37 percent) of its surface value. The following expression gives the relationship of the standard depth of induced current to the applied frequency [Bray and Stanley, 1997].

$$\delta = 50\sqrt{\rho/(f \cdot \mu r)} \quad [10]$$

where r is resistivity in $mW.cm$ and f is frequency in Hz . With changing frequency the hydrogen profile relative to the pipe surface can be assessed. Figure 7 illustrates the eddy current density as a function of depth. The skin depth relationship given in Equation 3.33 refers only to plane electromagnetic waves. In common eddy current testing situations, small coils or encircling tubes are utilized making Equation 10 invalid, but it does however provide a reasonable estimate of the skin depth [Bray and Stanley, 1997]. The skin depth relation is a solution to the Maxwell's equations, which should be determined for each particular inspection problem [Bray and Stanley, 1997].

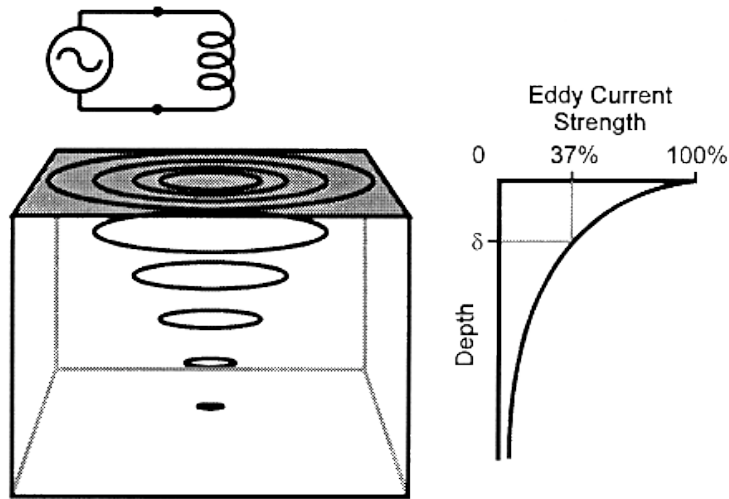


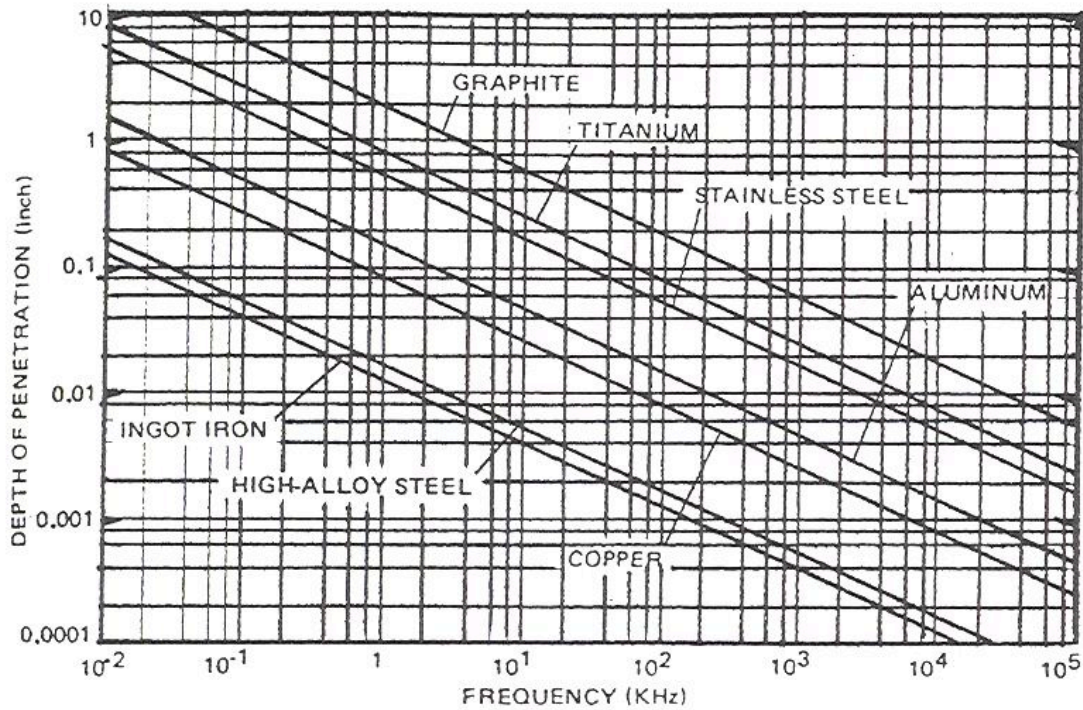
Figure 7: Schematic illustration of eddy current density declines with depth [Bray and Stanley, 1997].

Figure 8 shows the standard depth of penetration as a function of frequency for several different materials. Both permeability and conductivity play an important role in lowering the depth of penetration

[Bray and Stanley, 1997]. The resistivity is also temperature dependent, which also changes the depth of penetration.

Through thickness hydrogen measurements in the coated pipeline will require a large coil at a very low frequency (below 10 kHz). An eddy current unit is being specially designed to achieve these necessary low frequencies. This non-contact probe approach has high potential to determine the diffusible hydrogen content in a very convenient way.

Variables do exist in induced current resistivity measurements because resistivity is a function of the conductivity of the material, the depth of the measurement, and the alloy content. The conductivity is a function of the electronic effective mass, the electron concentration, and the dominating scattering mechanisms, which is altered by inclusions, microstructure, temperature, strain, and etc.



(a)

Figure 8: Standard depth of eddy current penetration versus frequency [Bray and Stanley, 1997].

New and Current Achievements in Induced Current Resistivity Measurements

Eddy current analyses have been taken beyond crack and defect detection to further monitor material properties before significant defects arise. Unfortunately, the development of eddy current analyses for

characterization of material properties has started out fairly slowly, but the extreme benefits in utilizing non-contact, non-destructive tools characterization of material properties is beginning to make an impact. The next section describes a new development of using eddy current analysis for carbon content detection.

Eddy Current Analysis for Carbon Content Measurements

Klumper-Westkamp et al. [2003] have utilized eddy current with harmonic analyses for non-destructive determination of carbon content in thin foils for quality assurance of gas carburizing process. Experiments were performed utilizing a set of 71 foils carburized with different carbon potentials and then analyzed for glow discharge emission spectroscopy element profiling and newly developed distortion free harmonic analysis. The system is calibrated utilizing multi-regression analysis. The input parameters are the amplitude and the phase of the first to the fifth harmonic of different frequencies, so that 36 measurements are available. By the connection of several measurements, the precision of the calibration is enhanced up to a correlation coefficient of 97.5 percent with a standard deviation of 0.06 weight percent carbon. The results are shown in Figure 9 for carbon concentration utilizing eddy current harmonic analysis as a function of carbon content from glow discharge emission spectroscopy. With more precise foil extraction the standard deviation would be even better.

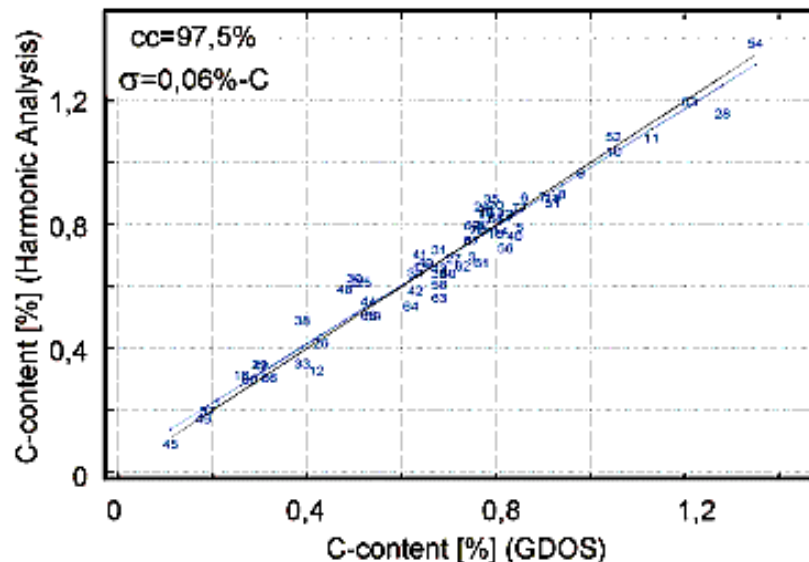


Figure 9: Calibration result for a 5-dimensional regression [Klumper-Westkamp *et al.*, 2003].

4. Experimental Plan

Development of a non-destructive tool to measure diffusible hydrogen in coated linepipe steel involves extensive calibration of the electromagnetic technique. The specimen preparation and calibration techniques are discussed in the below. X80 linepipe steel has been chosen as the candidate material to determine whether the electromagnetic tools can be utilized as a hydrogen sensor.

4.1. Specimen Preparation for Hydrogen Measurements

It is extremely important to note that all of the X80 linepipe steel specimens are machined from the same piece of linepipe steel and prepared identically to eliminate the introduction of any extra variables besides hydrogen content. In preparation for electromagnetic analyses, three large cylindrical specimens (5 mm diameter) and five small cylindrical specimens (3 mm diameter) as shown in Figure 10 are simultaneously hydrogen charged in a reactor at 400°C as a function of various times and pressures (100-1000 psig).



Figure 10: Photograph of uncoated X80 steel cylindrical specimens (large cylinder: 5 mm diameter and small cylinder: 3 mm diameter).

The large cylindrical specimen on the left (Figure 10) is used for electromagnetic analyses and the smaller cylindrical specimen on the right (Figure 10) is used for the determination of the total hydrogen content utilizing the Leco Hydrogen Determinator as shown in Figure 11. In the Leco Hydrogen Determinator, the sample is weighed and heated to about 300°C. The detector detects the hydrogen gas from the sample and plots it as a function of time. The amount of hydrogen is calculated from the area below the curve and reported in units of part per million compared with the weight of sample.

There are three large cylinders and five small cylinders hydrogen charged together in the same reactor, such that the large specimens are

used for repeatability of measurements and the five small cylinders are used to monitor hydrogen concentration changes over time.



Figure 11: Leco Hydrogen Determinator (www.leco.com).

The hydrogen charging system used in this investigation is shown in Figure 12 and 13. Both powder and bulk specimens can be hydrogen charged in this unit. Ultra high purity helium is used to clean the system before hydrogen charging of specimens. The system is evacuated until the pressure drops to 10^{-6} psi before hydrogen gas was input in the system. The hydrogen content in the metal is varied by the way of desorption and the Sieverts' law is applied to calculate the remaining hydrogen content. The equilibrium pressure of hydrogen gas is measured when the pressure remains constant at any hydrogen content during desorption for at least one minute [Termsuksawad *et al.*, 2005]. After charging LaNi_5 specimen with various levels of hydrogen as a function of time the specimens are quenched in cold-water to maintain the hydrogen in the specimens. If the specimen was allowed to cool in air, the hydrogen would diffuse back out of the specimen.

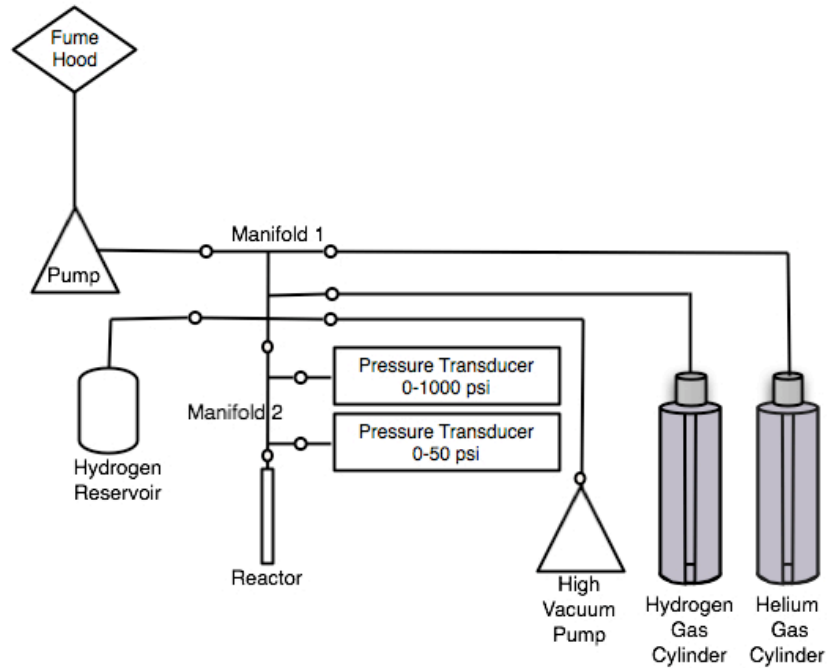


Figure 12: Hydrogen Charging System – A High pressure and high temperature hydrogen charging system.



Figure 13: High pressure and temperature hydrogen charging system.

After hydrogen charging the specimens at 400°C, the specimens must undergo an intermediate quench (dry ice and acetone) to maintain the

charged hydrogen content. If the sample was allowed to slowly cool to room temperature, most of the charged hydrogen will diffuse out of the specimen. After the intermediate quench, the specimens immediately undergo a hot tinning process. The hot tinning process is necessary to hinder the hydrogen from diffusing out of the steel specimens, so that when induced current impedance measurements were performed the hydrogen concentration was homogenous across the specimen. Note: Experiments were performed on numerous coatings to determine the best hydrogen barrier. A schematic diagram of the hot tinning process is shown in Figure 14. Each cylindrical specimen is individually removed from the intermediate quench and dipped into water to bring the specimen to room temperature, then submerged into the flux (which allows the tin to adhere to the steel) and finally the specimen is dipped into the first tin bath for ten seconds. It is next allowed to cool for approximately twenty seconds and then dipped into the secondary tin bath (which has mineral oil on the surface to allow for a nice finish). Normally, after the specimen has been dipped into the second batch of molten tin, there would be one more step to the process, which is an oil quench. When the specimens were oil quenched, the surface of the coating developed numerous distortions and defects. To minimize distortions in the coatings, the oil quench process was omitted and replaced with air-drying. A photograph of hydrogen-charged tin-coated specimens is shown in Figure 15. After the cylindrical specimens are tin-coated, the small cylinders are used for Leco Hydrogen Determinator Analysis (to track the estimated hydrogen in the large cylinders) and the large cylinders are used for electromagnetic analysis.

Experiments were also performed on uncoated hydrogen charged specimens to monitor the change in hydrogen as a function of time. Both impedance and thermoelectric power measurements are used for this study because contact can be made with the specimen surface.

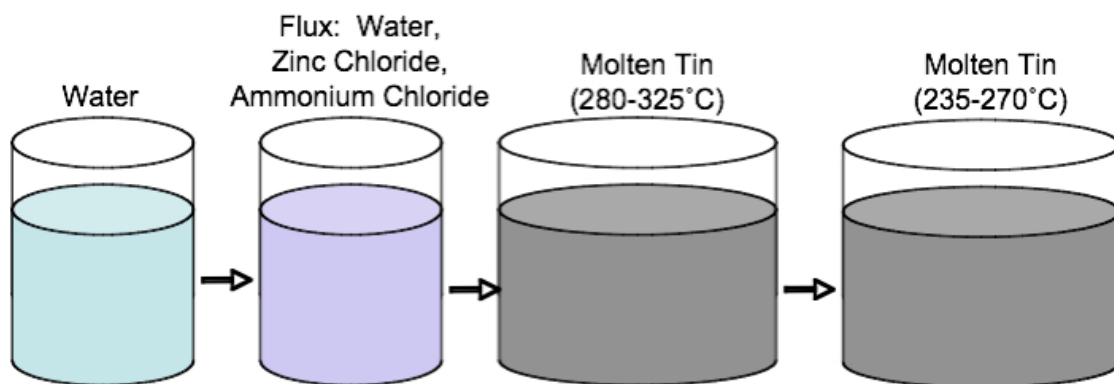


Figure 14: Schematic diagram for hot tinning of X80 steel specimens after hydrogen charging.

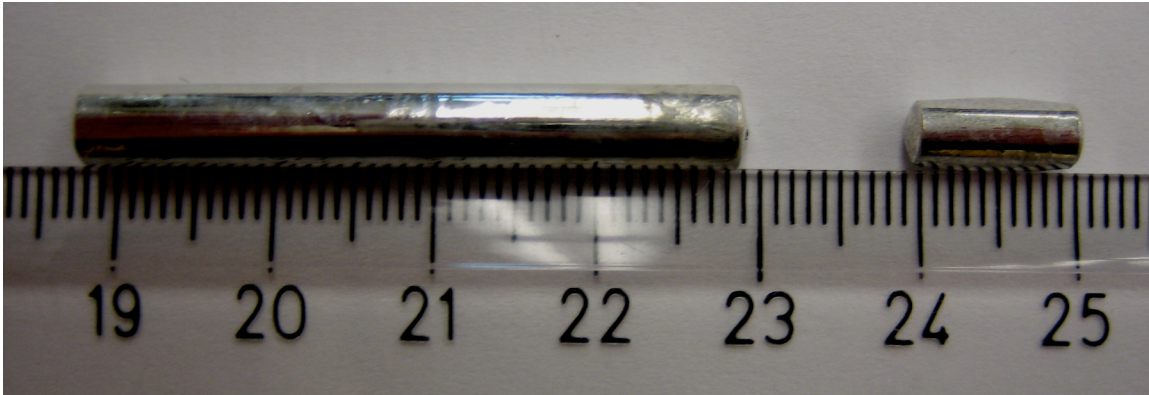


Figure 15: Photograph of tin-coated hydrogen charged X80 steel cylindrical specimens. The specimens are coated utilizing the hot tinning process shown in Figure 14.

4.2. Electromagnetic Probe Development for a Hydrogen Sensor

For generation and detection of eddy currents requires an oscillator, which is a means of generating a changing magnetic field close to the part, normally in the form of a coil, and a means of measuring the voltage in a detector. A Hewlett Packard 4275A Multi-Frequency LCR Meter (Figure 16) has the capabilities of inducing both the magnetic field and detection of voltage so that it can properly be utilized for electrical impedance measurements on hydrogen charged X80 linepipe steel specimens. Oscillation of the field is generally sinusoidal, with varying frequencies dependent upon the application and depth of measurement. For bulk hydrogen content measurements, low frequency measurements are necessary. Voltage measurements consist of amplitude and phase difference measurements from the exciter coil current. The eddy current coil sensors must be configured for the particular application.

The first step to attaining a good electromagnetic measurement is designing the proper probes to make such an analysis and the elimination of unnecessarily long wires (to reduce noise). For the first electrical impedance measurements, a simple cell was designed (at NIST) so that the tin-coated hydrogen-charged cylinder is sandwiched between two probes, each having an electrically-insulated alligator clip, as shown in Figure 17. One alligator clip is used to induce the current and the alligator clip at the opposite end measures the change in the induced current after it traverses across the specimen. This arrangement shown in Figure 16 is only used for initial experiments while the investigators are still determining the capabilities of the equipment. A copper coil probe (solenoid) has been designed such that there is a coil encircling the sample with a specific number of turns at specific lift-off as shown in

Figure 18. Rubber grommets are utilized to ensure a constant lift-off between the specimen and the coil.



Figure 16: Hewlett Packard 4275A Multi-Frequency LCR Meter utilized for electrical impedance measurements on hydrogen charged X80 linepipe steel specimens.

The magnetic field of a long solenoid, consisting of n closely wound turns per unit length on a cylinder of radius R and carrying a steady current I . If the turns per unit length are wound very closely, then it can be assumed that each turn is circular [Griffiths, 1999]. Ampere's law can be applied to calculate the magnetic field. The magnetic field inside the solenoid is calculated by:

$$\oint B \cdot dl = B\hat{z} = \mu_o I_{enc} = \mu_o nI\hat{z} \quad [11]$$

The magnetic field within the solenoid is uniform. Ampere's law is always true for steady currents, however it is not always the most useful equation. When Ampere's law does not work, it is necessary to fall back on the Biot-Savart law [Griffiths, 1999].

Utilizing the depth of penetration information from Figure 8, it is important to calculate the depth of the measurement in the cylindrical

X80 linepipe steel specimens. The depth of penetration in the cylindrical X80 linepipe steel specimen is on the order of 5 mm. A depth of penetration of 5 mm is quite good for hydrogen measurements because the measurement is not a skin affect and would be able to penetrate beneath a coating. To increase the depth of penetration, the number of windings in the copper coil can be increased.

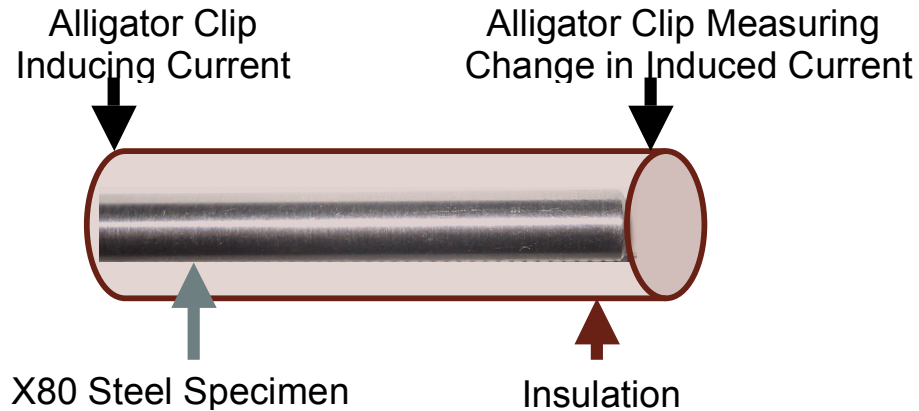


Figure 17: Schematic diagram illustrating an arrangement for inducing and measuring current. The alligator clips are connected to the insulation and make no electrical contact to the cylinder.



Figure 18: Photograph of the encircling coil utilized for impedance measurements. Rubber grommets are utilized to guarantee constant lift-off between the specimen and the copper coil.

After determining the effect of hydrogen on impedance, the coil sensitivity will be investigated and the induced magnetic field varied. Coils were designed with variable number of turns, two different wire gauges, and different configurations. To test the capability of each coil, a single hydrogen-charged cylindrical X80 linepipe steel specimen was

prepared and used for testing each coil. The different coils utilized in this experiment are shown in Figure 19. For each coil, measurements of impedance, resistance, and inductance were conducted. The inductance was measured for each coil because the inductance is purely a geometrical quantity dealing with sizes, shapes, and positioning of coils. When the current changes, the electromotive force induced into the coil also changes. Coils G-1 through G-5 are encircling coils and coils G-6 and G-7 perform measurements near the surface. G-6 and G-7 coils were used in the flat (or pancake) position and spread-out as shown. A square Litz wire was also investigated.

Litz wire is designed to minimize the power losses exhibited in solid conductors due to "skin effect". Skin Effect is the tendency of radio frequency current to be concentrated at the surface of the conductor. Litz constructions counteract this effect by increasing the amount of surface area without significantly increasing the size of the conductor. Generally speaking, constructions composed of many strands of finer wires are best for the higher frequency applications, therefore Litz construction is not optimal for the low frequency application necessary for bulk hydrogen measurements.

Another coil study was also performed using both a pancake and encircling coil on X80 cylindrical specimens that have undergone heat treatment. Heat-treated specimens were chosen because the coils need to be very sensitive to measure changes in microstructure because the impedance values will be performed where the hydrogen content is approximately zero. The impedance values are very low when the hydrogen content is low, so it will be interesting to see if either or both of the probes will see a change in microstructure.



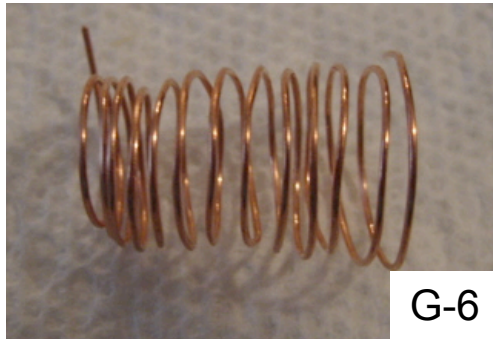
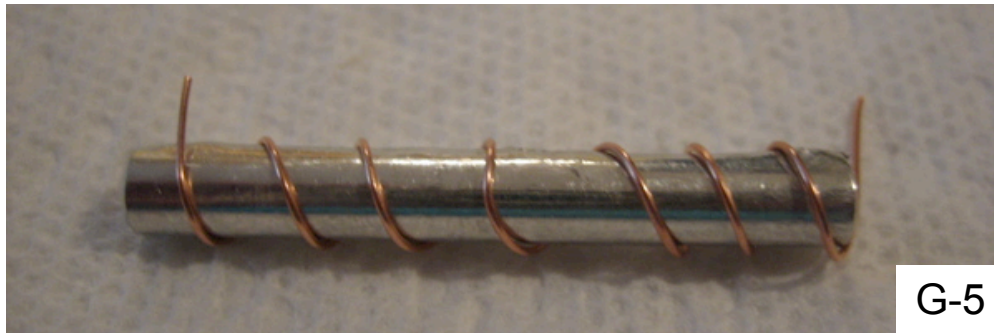


Figure 19: Variable copper coil arrangements for impedance analysis.

4.3. *Electromagnetic Sensor Development for Temperature and Microstructure Corrections*

In the beginning of the project it seemed that it would be necessary to utilize multiple techniques to eliminate variables associated with the pipeline, however it was found that induced current impedance measurements may be able to perform the same measurements. The use of a single tool to measure hydrogen content while accounting for all

variables will make this technique more cost and time efficient. Also, the magnetic remanence present in the pipeline leftover from pigging operations would interfere with magnetic Barkhausen noise measurements for microstructure characterization, thus increasing the importance of the development of a tool successful for full material characterization.

4.3.1. Specimen Preparation for Temperature Measurements

To correct for variations in temperature in pipelines, induced current impedance analysis was investigated to determine the effect of temperature on impedance. X80 steel linepipe specimens used in the hydrogen investigation above were utilized again. The specimens were not hydrogen charged for this investigation. X80 linepipe steel cylindrical specimens were held at various temperatures and allowed to cool/heat as a function of time while measuring the change in impedance. Also the impedance as a function of time was measured at different temperatures to determine the sensitivity of impedance to temperature.

4.3.2. Specimen Preparation for Microstructure Measurements

To correct for variations in microstructure in pipelines (X65 versus X80, X100, etc.) impedance analysis was also utilized. To determine the sensitivity of impedance for microstructure various linepipe steel specimens were collected and compared. Unfortunately at this time, only two different linepipe steels were received which were X80 and X100. So, to verify the sensitivity of impedance to microstructure, specimens were prepared from the X80 linepipe steel by heat-treating the specimens at different temperatures at quenching them by water quenching, oil quenching, or air-cooling. One set of specimens experienced a heat treatment of 400°C and the other set at 900°C. Each of these annealing and cooling techniques promotes variable microstructures to allow for a microstructure impedance investigation.

A set of eight different specimens machined from the same piece of linepipe steel were also investigated with impedance measurements to determine whether or not there was any variance between the initial (standard) specimens cut from the X80 linepipe steel. This experiment guarantees the accuracy in the results because these specimens act as standards and should be fully characterized.

4.4. Low Frequency Impedance Through a Coating

Techniques to eliminate variables in hydrogen content measurements have been discussed, so that the only factor remaining is performing low frequency impedance measurements through a coating. For this experiment an epoxy coating is utilized as seen in Figure 20. The specimen was put into a Petri dish and the dish was then filled with epoxy and allowed to dry completely. It is important to make sure that the epoxy was filled to the top of the dish and made as uniform as possible. A second sample is put into another Petri dish without a coating. The Petri dish is important because it will provide a means of measuring a constant lift-off between a specimen with a coating and without a coating. Otherwise, the lift-off due to the coating compared to an uncoated specimen would not allow measurements to be correlated to one another.

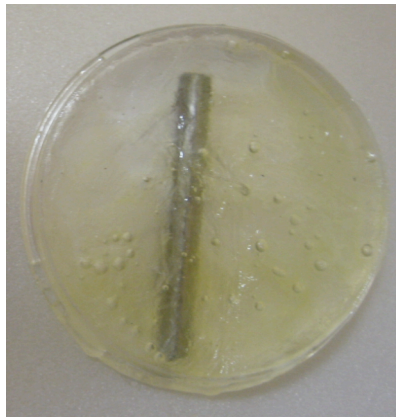


Figure 20: X80 cylindrical specimen in Petri dish surrounded by an epoxy coating.

5. Experimental Results

Electromagnetic analyses have been developed for determination of hydrogen content in coated X80 linepipe steel specimens. The electromagnetic analyses allows for a non-destructive, non-contact means for hydrogen content determination. The experimental results in the development of a hydrogen sensor are given below.

5.1. Electromagnetic Hydrogen Sensor

A frequency sweep was performed on cylindrical steel specimens that were hydrogen charged to different levels of hydrogen by varying the charging time and pressure held at a temperature of 400°C (hydrogen content being the sole variable) to determine if there were any measurable changes in impedance as a function of the hydrogen content.

The cylindrical X80 steel linepipe specimens, which underwent the electromagnetic analyses, had total hydrogen contents ranging from 0.78 to 23.1 ppm of hydrogen determined by the Leco Hydrogen Determinator.

The initial results for the change in impedance due to changes in hydrogen content as a function of frequency is given in Figure 21. The impedance is then plotted as a function of hydrogen content at approximately 100 Hz (depth of 5 mm) as shown in Figure 22. The results are most important at lower frequencies (Log Frequency = 2 Hz) to guarantee a maximum penetration depth of 5 mm beneath the surface. At frequencies beyond 100 Hz (> Log Frequency = 2 Hz) only skin effects (the specimens are coated with tin barrier) are being monitored, which cannot be attributed to variations in hydrogen content but variations in the coating, etc.

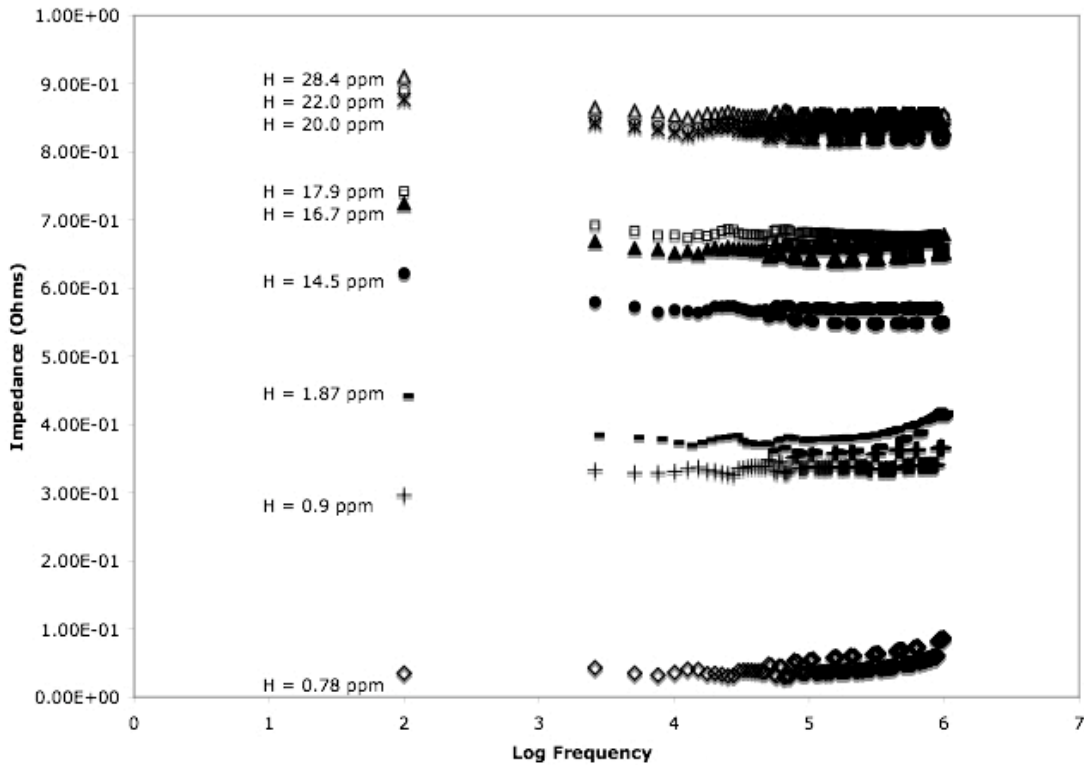


Figure 21: Frequency sweep of impedance with change in hydrogen content in tin coated hydrogen charged X80 steel specimens. Impedance measurements were performed utilizing the Hewlett Packard 4275A Multi-Frequency LCR Meter.

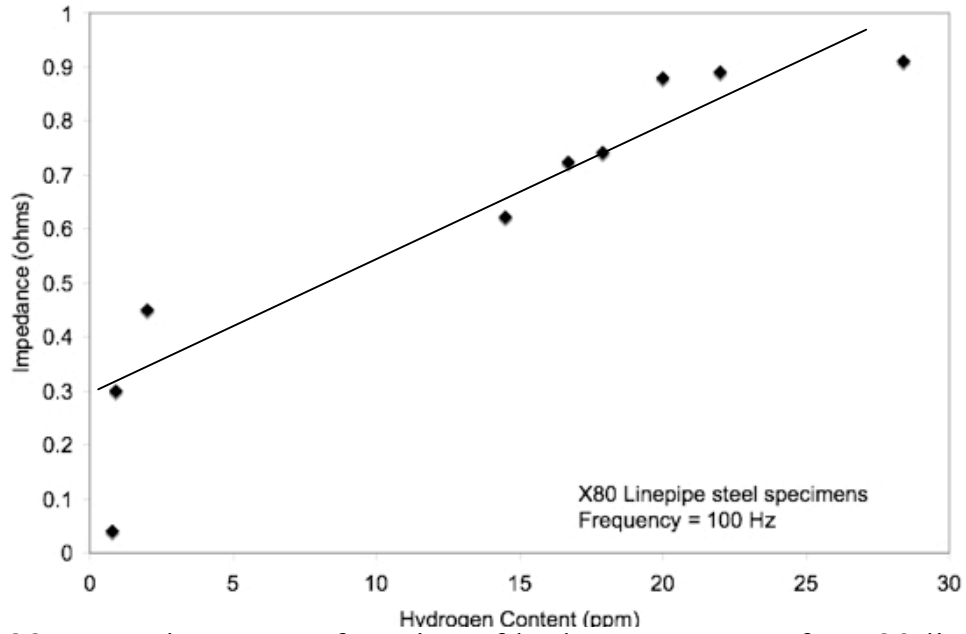


Figure 22: Impedance as a function of hydrogen content for X80 linepipe steel specimens at frequency of 100 Hz.

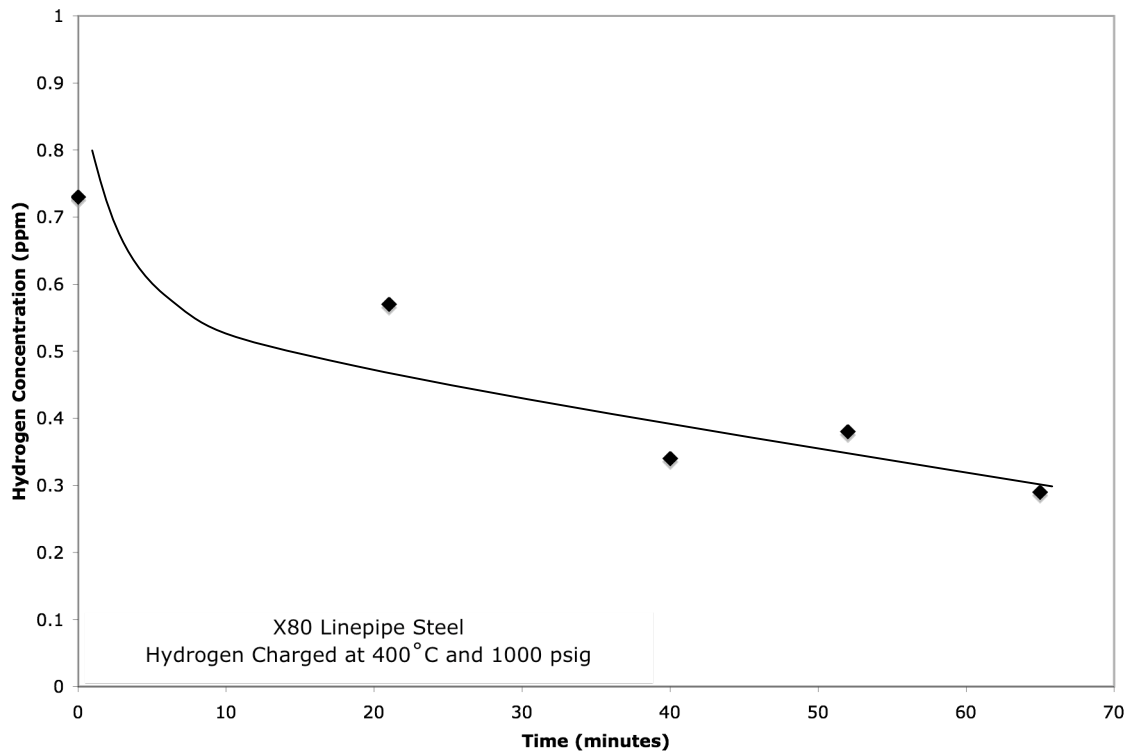


Figure 23: Hydrogen content as a function of time for hydrogen diffusion in hydrogen charged X80 steel linepipe specimens.

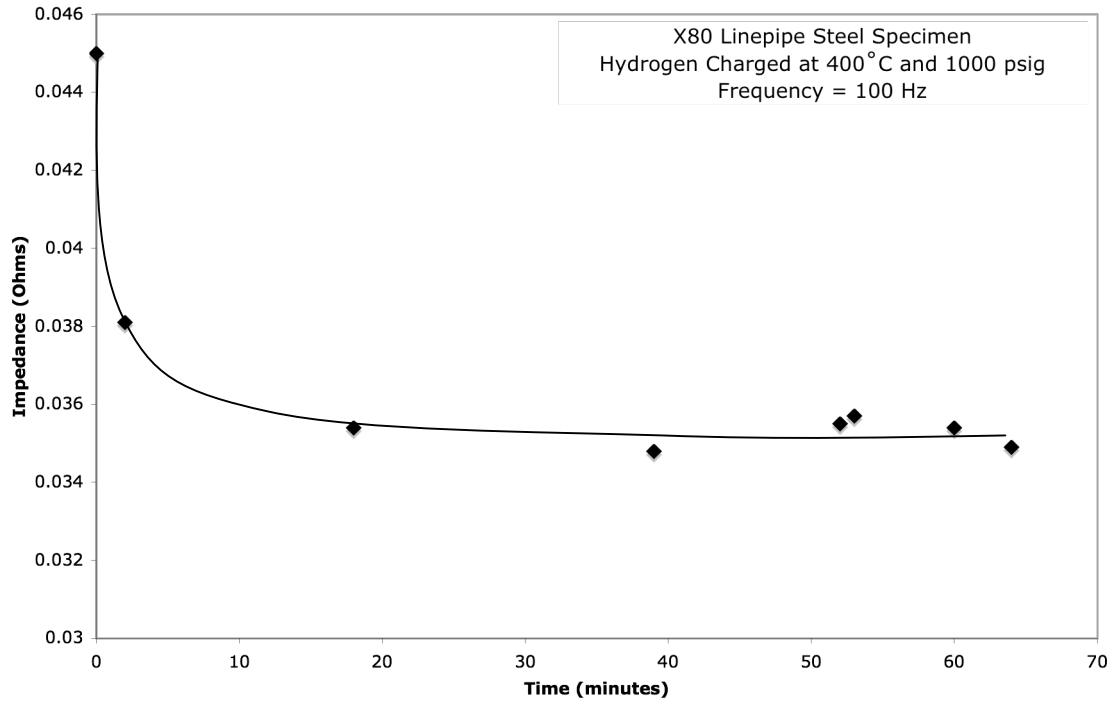


Figure 24: Change in impedance as a function of time for uncoated hydrogen charged X80 linepipe steel specimens.

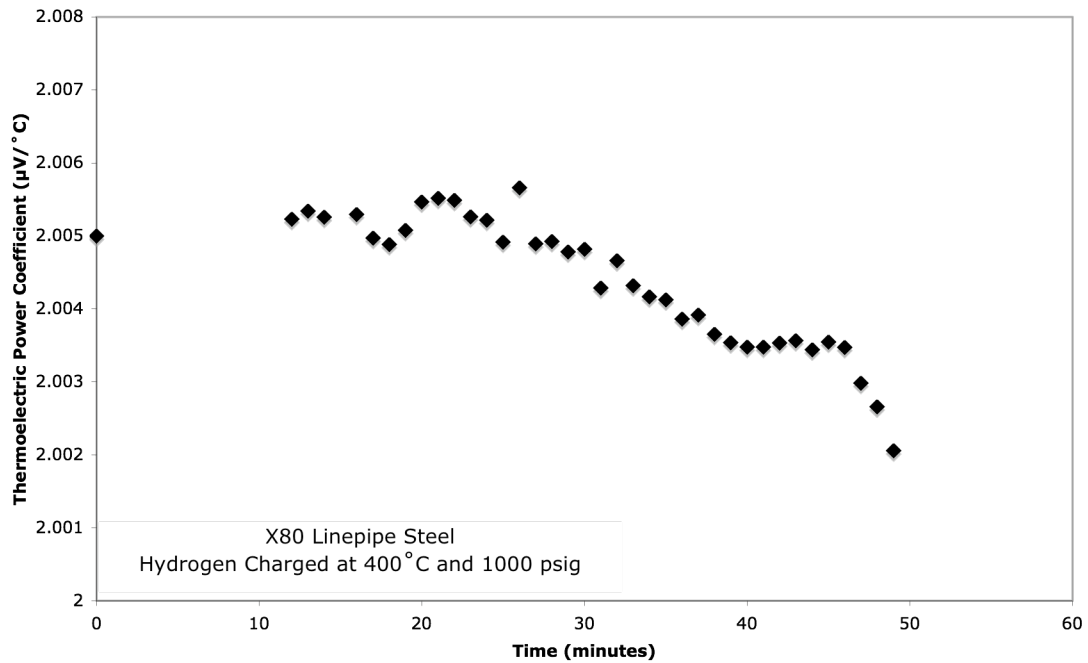


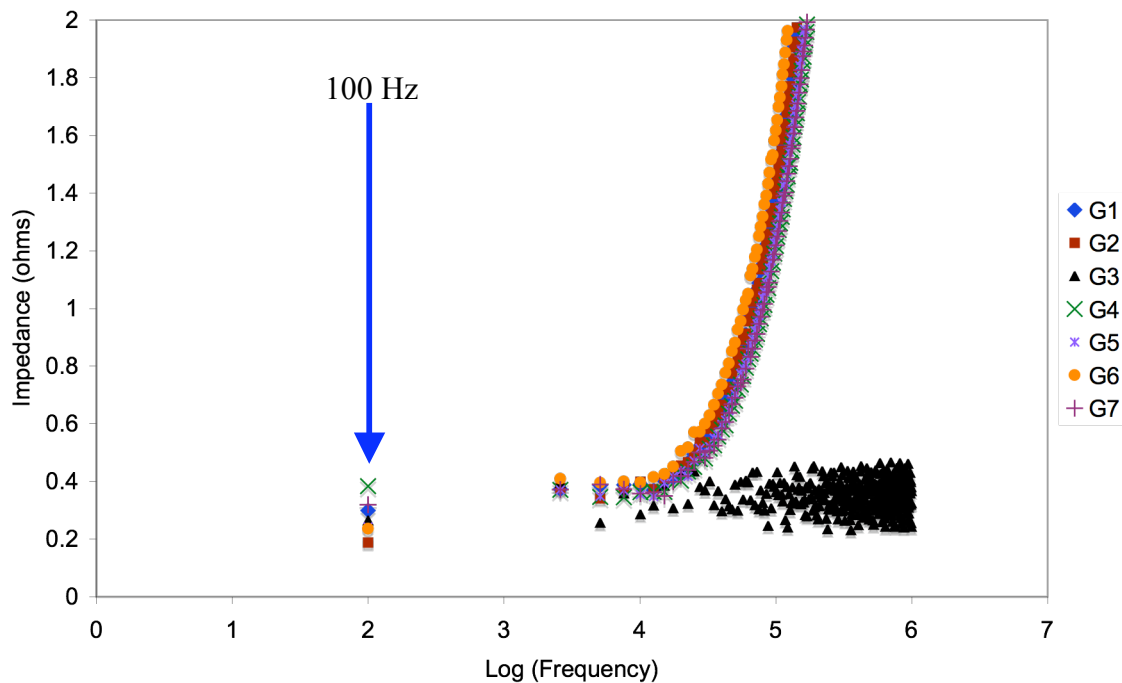
Figure 25: Change in thermoelectric power coefficient as a function of time for uncoated hydrogen charged X80 linepipe steel specimens.

5.2. Electromagnetic Coil Development

Development of the electromagnetic coil is important to maximize the depth of impedance measurements to achieve bulk hydrogen measurements. Table 1 lists the results for the various coil configurations. Figure 26 (a) shows the frequency sweep impedance comparison for each coil utilized. Figure 26 (b) is a closer look at the results from part (a) showing the variation between impedance for each coil at specifically 100 Hz.

After an initial comparison of data for different coils, a pancake coil (wire gauge of 18 and 7 coil turns) and an encircling coil (wire gauge of 18 and 7 coil turns) were compared on three different samples with different heat treatments and cooling as shown in Figures 27, 28, and 29.

Sample	Wire Gauge	Number of coil turns	Frequency (Hz)	Impedance	Inductance	Resistance
G1	24	23	100	0.299	-1.94E-4	0.307
G2	24	45	100	0.188	7.29E-5	0.475
G3	18	29	100	0.401	1.35E-4	0.534
G4	18	9	100	0.384	-2.57E-4	0.213
G5	24	7	100	0.242	-1.26E-4	0.193
G6	24	13	100	0.237	1.38E-4	0.305
G7	18	7	100	0.319	1.66E-4	0.438



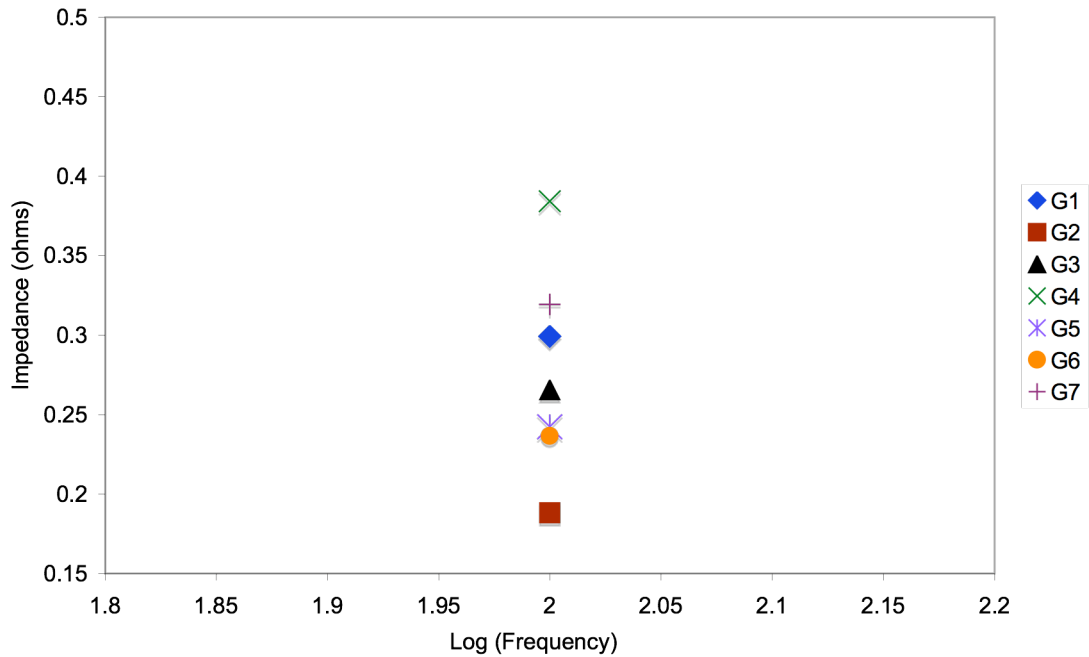


Figure 26: (a) Frequency sweep for different coils configurations on X80 linepipe steel specimens (b) Comparison of impedance for each coil at 100 Hz.

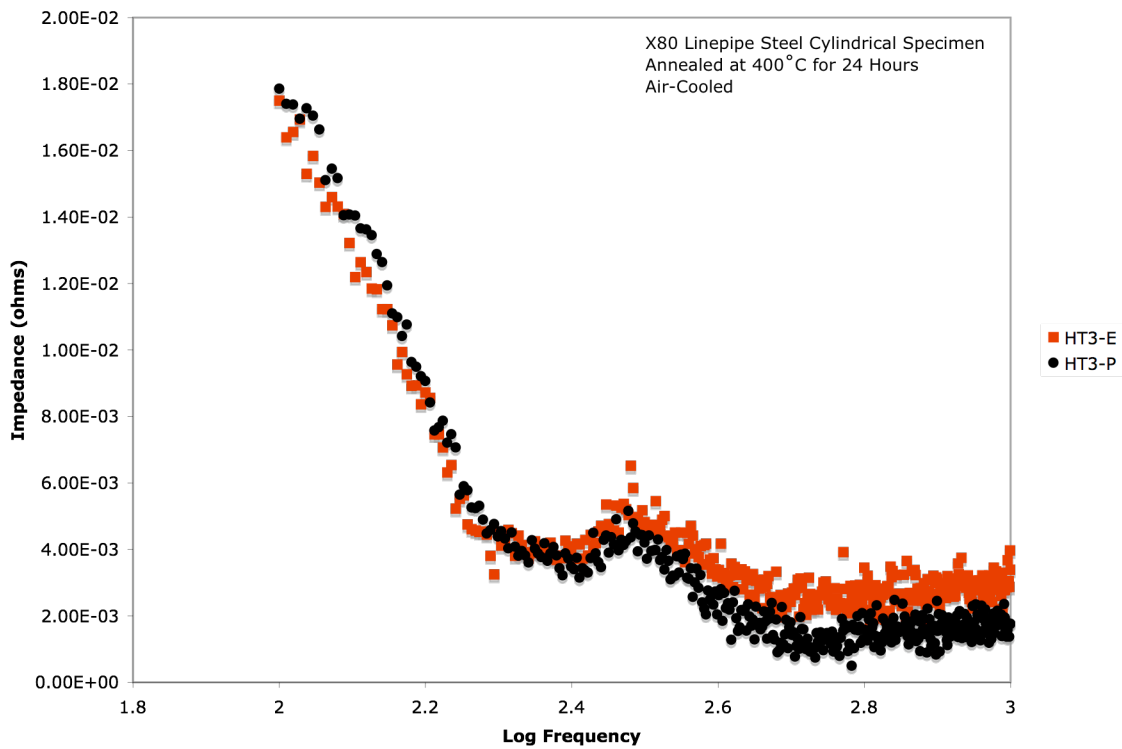


Figure 27: Impedance as a function of frequency utilizing an encircling coil and a pancake coil for X80 cylindrical specimen heat-treated for 24 hours at 400°C and then air-cooled.

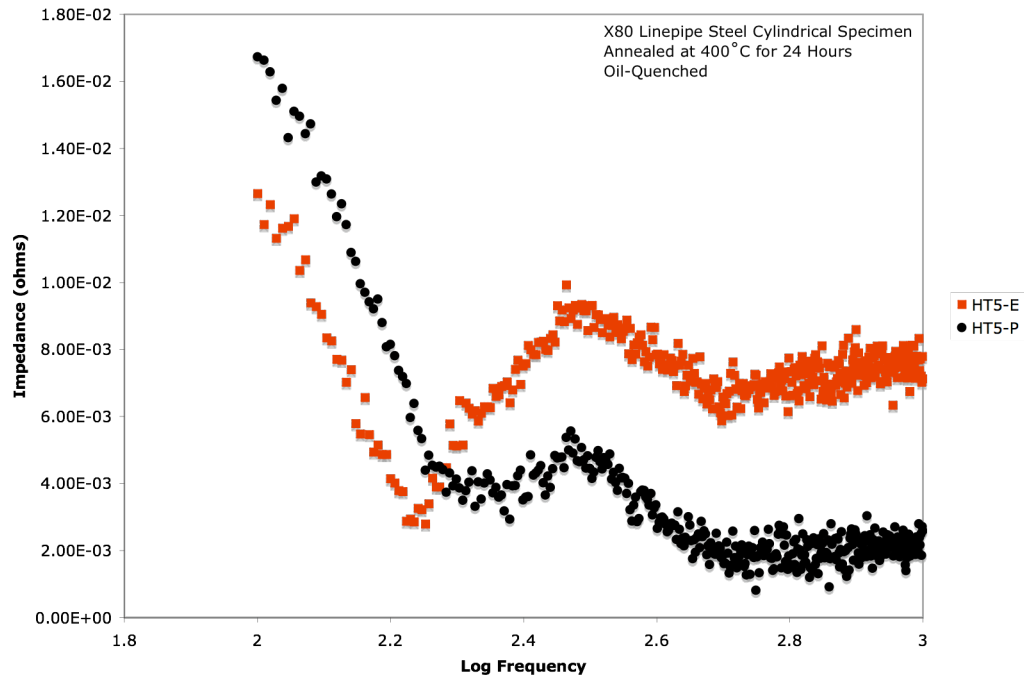


Figure 28: Impedance as a function of frequency utilizing an encircling coil and a pancake coil for X80 cylindrical specimen heat-treated for 24 hours at 400°C and then oil quenched.

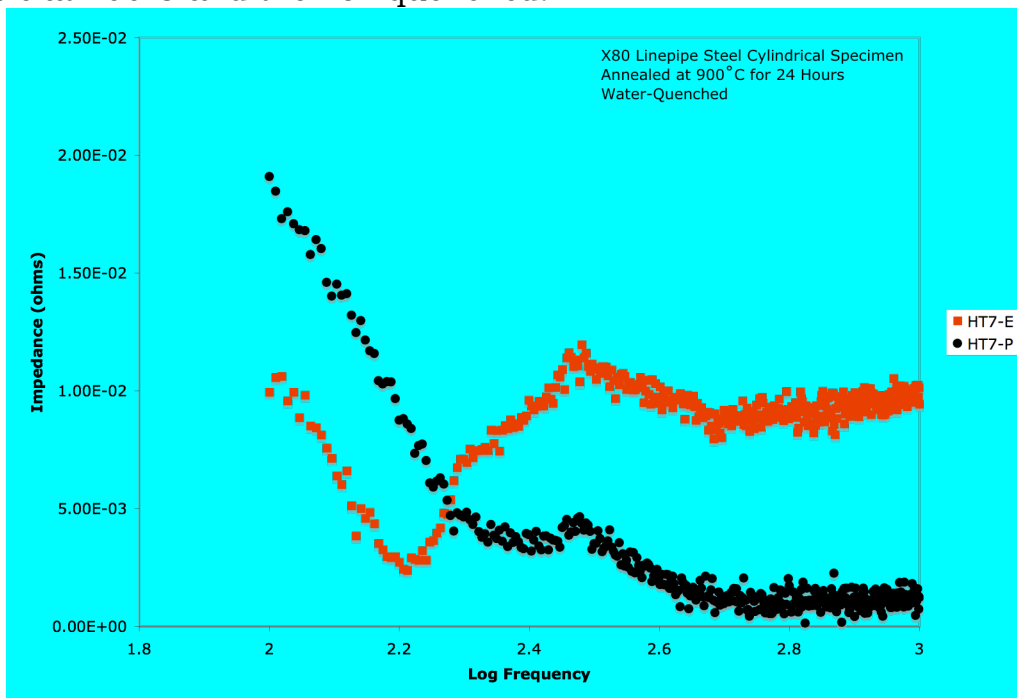


Figure 29: Impedance as a function of frequency utilizing an encircling coil and a pancake coil for X80 cylindrical specimen heat-treated for 24 hours at 900°C and then water-quenched.

5.3. *Electromagnetic Temperature Measurements*

Results indicating change in impedance as a function of time during heating of X80 linepipe steel specimens at a frequency of 100 Hz is shown in Figure 30. Figure 31 then shows a comparison of impedance for various temperatures at a frequency of 100 Hz.

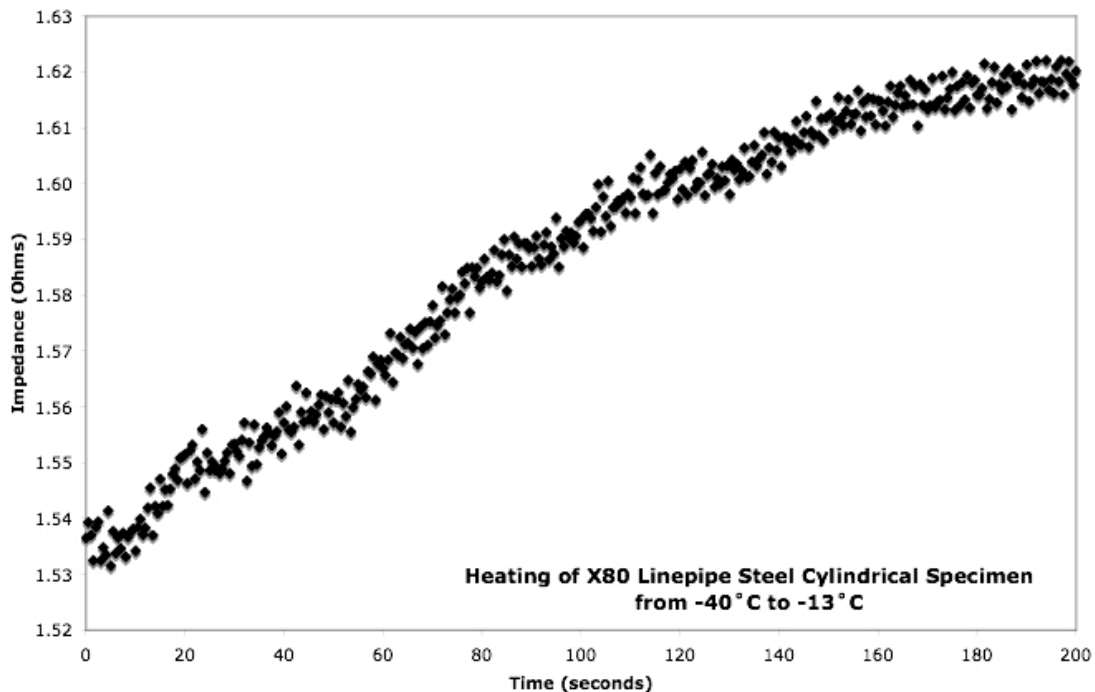


Figure 30: Impedance as a function of time measured while heating X80 linepipe steel specimens from -40°C to -13°C at a frequency of 100 Hz.

5.4. *Electromagnetic Microstructure Measurements*

A comparison was made in the impedance for X80 and X100 linepipe steel specimens as shown in Figure 32. Figure 33 shows the change in impedance as a function of time for various X80 specimens, which underwent different heat treatments and types of quenches to provide microstructural variations. Using heat treatments as a variable will show the sensitivity in impedance measurements versus the difference in two different grades of steel, which should have a measurable difference.

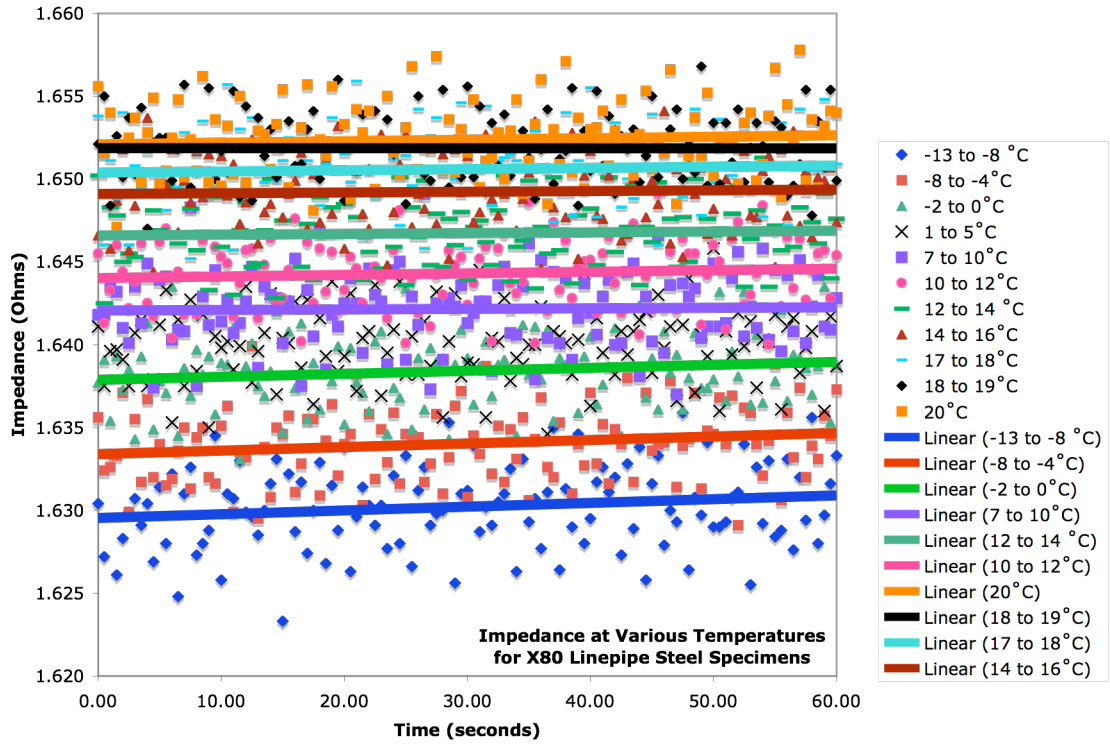


Figure 31: Impedance as a function of time for X80 linepipe steel specimens held at various temperatures at a frequency of 100 Hz.

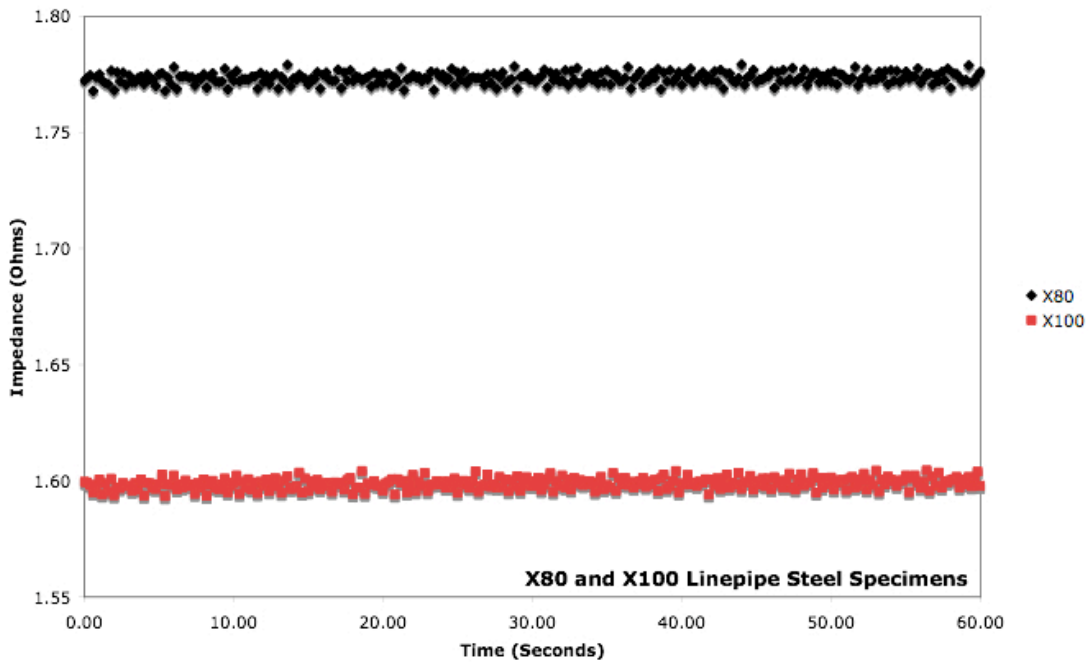


Figure 32: Comparison of impedance as a function of time for X80 and X100 linepipe steel specimens.

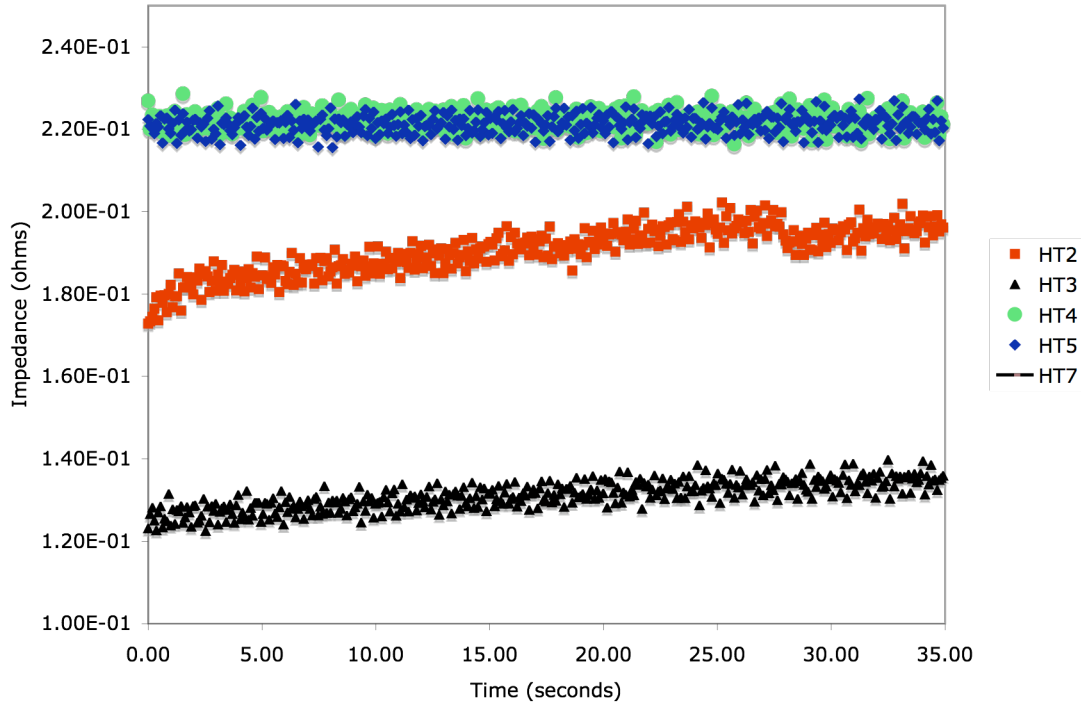


Figure 33: Comparison of impedance as a function of time for heat-treated X80 linepipe steel specimens.

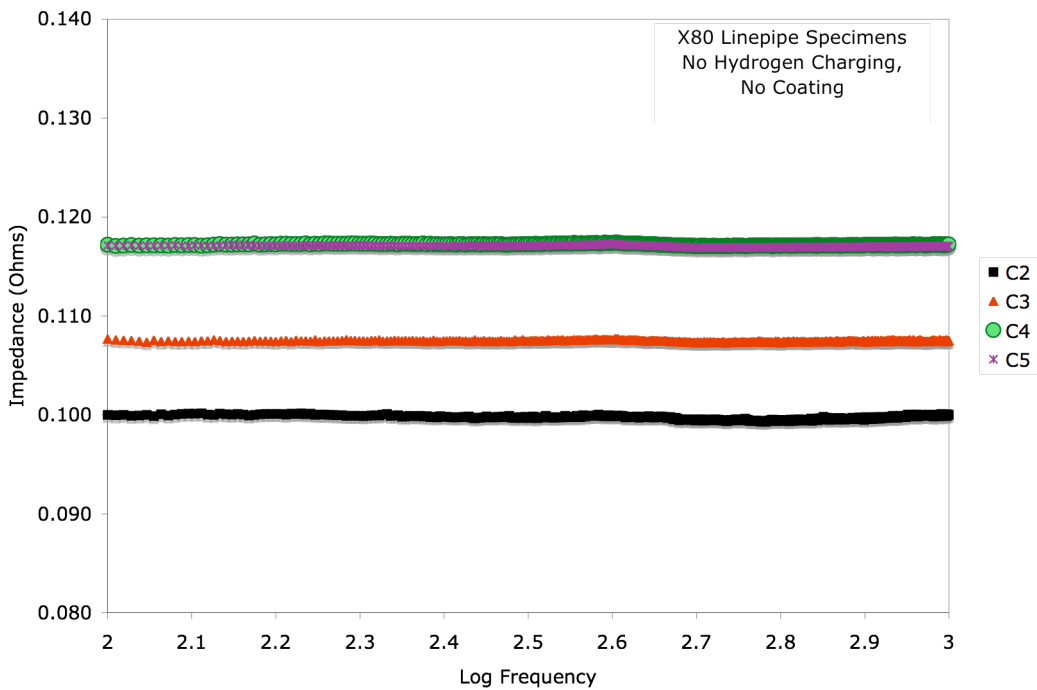


Figure 34: Impedance as a function of frequency for four X80 cylindrical specimens machined from the same material with the only variable being machining of the samples to determine the variance between each sample.

5.5. Low Frequency Impedance Measurements Through a Coating

To utilize low frequency impedance measurements on a coated pipeline, it was necessary to determine whether impedance measurements changed on identical specimens with and without a coating. Figure 35 is a plot of impedance as a function of frequency. Three different conditions are shown in this plot: (1) impedance on a coil without a specimen, (2) impedance on a sample without a coating at a specific lift-off, and (3) impedance on a sample with a coating with a specific lift-off to match condition 2.

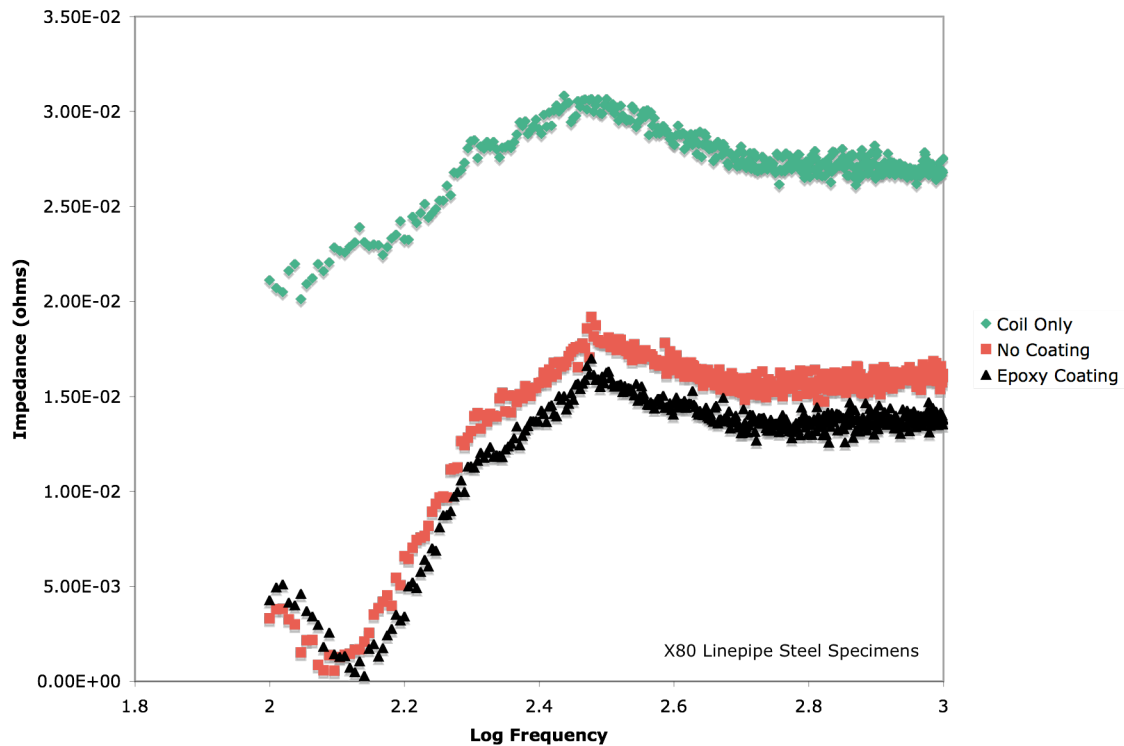


Figure 35: Impedance as a function of frequency for coated and uncoated X80 steel cylindrical specimens.

6. Analysis of Results

6.1. Electromagnetic Hydrogen Sensor

In Figure 21, notice how the impedance as a function of frequency increases with increasing hydrogen content. Not only are there measurable changes in impedance, but the sensitivity of the impedance measurements is exceptional. It cannot only measure hydrogen below 1.0 ppm, but it can also distinguish between 0.76 and 0.90 ppm of hydrogen. As the steel strength increases, the tolerance for hydrogen

approaches these small hydrogen contents. These low levels of hydrogen detection are within the uncertainty of chemical methods, but appear to be clearly measurable with physical electromagnetic tools. These preliminary results utilizing induced current impedance measurements demonstrates that it is feasible to develop electromagnetic (eddy current) measurements to assess hydrogen in line pipe steel. The impedance results in Figure 22 show the increasing trend of impedance as a function of hydrogen content. In Figure 21, notice how the impedance as a function of frequency increases with increasing hydrogen content. Not only are there measurable changes in impedance, but the sensitivity of the impedance measurements is exceptional. It cannot only measure hydrogen below 1.0 ppm, but it can also distinguish between 0.76 and 0.90 ppm of hydrogen. As the steel strength increases, the tolerance for hydrogen approaches these small hydrogen contents. These low levels of hydrogen detection are within the uncertainty of chemical methods, but appear to be clearly measurable with physical electromagnetic tools. These preliminary results utilizing induced current impedance measurements demonstrates that it is feasible to develop electromagnetic (eddy current) measurements to assess hydrogen in line pipe steel.

The measured impedance is a function of both the resistance and reactance. Capacitance does not play a significant role in the impedance measurements because very short wires (2.5 inches) were used in the measurements. To develop an understanding of how impedance measurements can detect changes in hydrogen content it is necessary to closely look at each individual term in the impedance.

Inductive reactance makes a small contribution to the impedance at low frequencies used in these experiments. A frequency of 100 Hz provided the maximum depth of penetration. The contribution of inductive reactance increases with increasing frequencies, thus the inductive reactance plays a larger role (but not a very large role relative to the resistance) in the overall impedance at higher frequencies as shown in Figure 22.

The resistance term from Equation 8 is more closely examined. The resistance is given as:

$$R = \frac{\rho l}{A} \quad [12]$$

where ρ is resistivity, l is the length of the specimen, and A is the area of the specimen. For a cylinder in an induced magnetic field, the resistance is not only inversely proportional to the area of the specimen, but the frequency being a function of depth must be accounted for in the area term. As discussed earlier, at low frequencies, flux is being generated in a greater specimen depth as opposed to higher frequencies where the

flux is generated only at the surface of the specimen. So accounting for the depth of measurement as a function of frequency, the area is proportional to:

$$A \propto \frac{A_o}{(\omega + 1)^{1/2}} \quad [13]$$

where A_o is the real cross-sectional area of the specimen and A is the actual area of the specimen being induced with currents. Then the resistance can be written as:

$$R = \frac{\rho l (\omega + 1)^{1/2}}{A_o} \quad [14]$$

The net resistivity must also be considered when determining the change in resistance due to the addition of hydrogen atoms. The resistivity change arises from independent scattering processes, which according to Matthieson's rule are additive. For dilute solutions, Matthieson's rule is in excellent agreement with experiments as shown for copper in Figure 36 [Wilkes, 1973]. Not only does Figure 36 show the effect of temperature on resistivity, but it also shows the effect of alloying elements on resistivity.

The net resistivity is then given as:

$$\rho_{net} = \rho_{lattice} + \rho_{thermal} + \rho_{Hydrogen} [H] \quad [15]$$

where $\rho_{lattice}$ is scattering due to grain boundaries, defects, and other phenomena in the lattice, $\rho_{thermal}$ is thermal scattering due to temperature, and $\rho_{hydrogen}$ is the change in resistivity due to the addition of hydrogen atoms. When a hydrogen atom in solution is entered into the metal, it also acts as a source of scattering, which arises from a departure from regularity in the ion lattice. The scattering due to the hydrogen atoms is independent of thermal scattering. In these experiments, the thermal resistivity can be neglected because the temperature is held constant.

Accounting for the net resistivity and the angular frequency, the resistance can now be re-written as:

$$R = \frac{(\rho_l + \rho_t + \rho_H [H]) l (\omega + 1)^{1/2}}{A_o} \quad [16]$$

When measuring the flux at full depth, the area is the cross-sectional area of the specimen. When the angular frequency goes to zero (the point where ac goes to dc), the resistance is given as:

$$R = \frac{(\rho_l + \rho_t + \rho_H[H])l}{A_o} \quad [17]$$

Notice this relationship between resistivity and hydrogen as shown in Figure 36 by recognizing the systematic increase of the intercept of the various copper content lines. With all things being held constant within the specimens as shown in Figure 37, the variations in hydrogen content are monitored due to the change in scattering or resistivity due to the departure from regularity in the crystal lattice.

When considering the effects of the net resistivity due to the lattice (defects, grain boundaries, etc.), temperature, and hydrogen, notice in Figure 37 how the resistivity due to hydrogen content is a function of the slope of the line and therefore the resistivity due to temperature and lattice variables may be accounted for in the y-intercept. Using this information, it may be possible to calibrate specimens with temperature and lattice as variables utilizing the same induced current impedance measurements as used for hydrogen content determination. This finding is important because it would be more efficient to be able to eliminate the variables in the pipelines by utilizing one single technique. To calibrate induced current impedance measurements for temperature and lattice variations, cylindrical specimens would be made and impedance measurements would be performed at various temperatures and on numerous microstructures (various X80 microstructures).

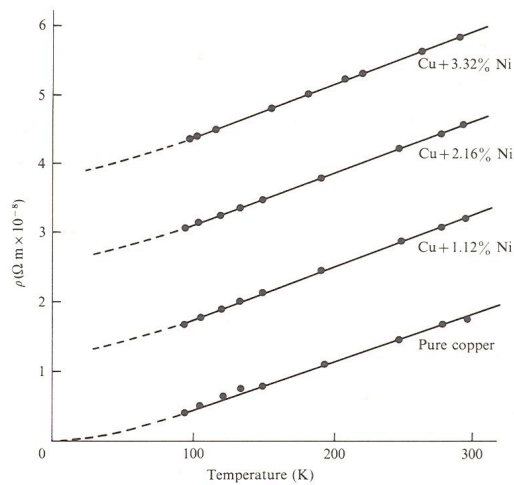


Figure 36. Temperature variation of resistivity for copper and copper alloys [Linde, 1932], [Wilkes, 1973].

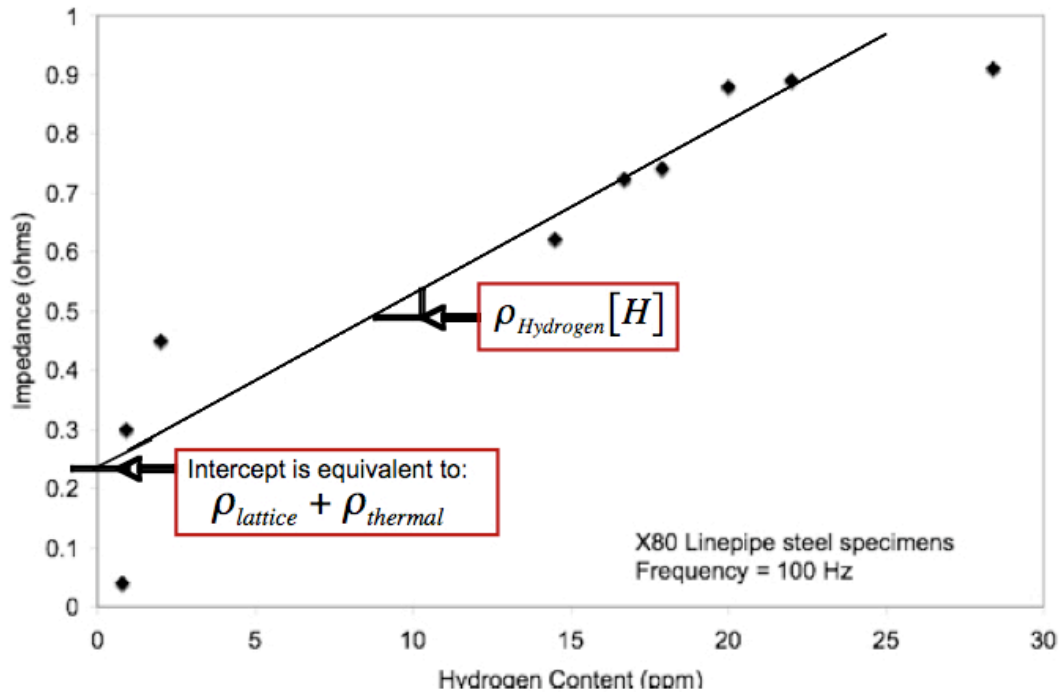


Figure 37. Induced current measurements as a function of hydrogen content at a frequency of 100 Hz showing where the resistivity of hydrogen is the slope of the line and the y-intercept is the resistivity of temperature and lattice.

The results shown in Figure 23, 24, and 25 also show that both thermoelectric power and impedance measurements are very sensitive to changes in hydrogen content as a function of time. These results are very important because both measurements (thermoelectric power and impedance) can be utilized to monitor changes in hydrogen content as a function of time in pipelines. The thermoelectric power technique could be installed into a new pipeline being developed or impedance measurements can be utilized on existing pipelines where measurements must be made through coatings.

6.2. Electromagnetic Coil Development

The development of the electromagnetic coil has proven to be an extremely important task. The change in coil design affects the overall impedance and resistance. The maximum inductance was achieved in specimen G7, a pancake type coil with the gauge size of 18 and only 7 turns. This pancake coil is preferred because it is not an encircling coil,

making measurements easier by allowing the user to be able to approach a coated pipeline and perform measurements.

The experiments performed with different electromagnetic coils also indicated the variance in impedance, which is important for calibration and standardization. The coil utilized in field use will have to be the same coil utilized when making standards. In other words, each coil will have to have its own set of calibration curves and standards.

Lift-off is another important factor. The variation in coating thickness must be accounted for to achieve an accurate hydrogen measurement. The same impedance analyzer can be utilized to determine the thickness of the coating. It is necessary to properly adjust to achieve the lift-off for which a set of standards is calibrated. Another way to eliminate lift-off effects would be to make calibrations at various lift-offs, but the coating thickness would still need to be accurately determined.

The impedance results in Figure 27, 28, and 29 utilizing a pancake coil and encircling are important in that they show that both coils can be utilized to measure very small changes in microstructure, and thus impedance. The results also show that the pancake coil may be a bit more sensitive to the microstructure changes, which agrees with the previous coil results in Figure 26.

6.3. *Electromagnetic Temperature Sensor*

Low frequency impedance analysis was used to determine the sensitivity of impedance to temperature variations. It was already known that resistance and thus impedance is sensitive to temperature as shown in Figure 36 by other researchers, however it was necessary to determine how sensitive impedance is to temperature. Figure 30 has a temperature range of -40 to -13 °C with measured impedance spanning from 1.53 to 1.63 Ohms. This data shows the level of sensitivity of impedance to temperature, which is very good. The impedance variation with temperature has a large enough difference that calibration of impedance with temperature is and will be very successful. Results in Figure 31 measured the change in a specific temperature range as a function of time. It also shows the sensitivity of temperature measurements utilizing low frequency impedance measurements.

6.4. *Electromagnetic Microstructure Sensor*

Low frequency impedance measurements were performed to determine the sensitivity of impedance to variable microstructures. Only two different types of pipeline steels were obtained at this time, however the results shown in Figure 32 for X80 and X100 show that there is a significant difference in impedance between the two pipe steels. To create variables in microstructure five different X80 specimens

underwent annealing and quenching. Figure 33 shows that impedance is also sensitive to these small changes in microstructure as would be expected because impedance measures any changes in grain size (due to flow of current).

To guarantee that the differences seen between the variable microstructures was an effect due to the annealing process, five different specimens with the only variable being machining and location of machining was analyzed as shown in Figure 34. These results are very important to show the scatter between each individual specimen. This experiment should be performed before each and every test especially when performing calibrations and standards. The data in Figure 34 showed that the standard deviation between samples is approximately 0.8%, which is acceptable considering the measured changes in impedance in all of the testing. These results also mean that the variation between measurements for example with variable microstructure is due to microstructure and not unforeseen pre-existing variables within the specimens.

6.5. Low Frequency Impedance Measurements Through a Coating

The low frequency impedance measurements performed on coated X80 cylindrical specimens is the final necessary link in utilizing impedance measurements for hydrogen sensing in pipelines. The results in Figure 35 compared the impedance as a function of frequency for a coated (epoxy) and uncoated specimen. The impedance as a function of frequency at 100 Hz are extremely similar. The standard deviation between the impedance of the two specimens is approximately .06%, which indicates that low frequency impedance measurements can successfully perform measurements through a coating. Also notice the values of the impedance for the coils in Figure 35. The values are over an order magnitude lower than the impedance as a function of hydrogen measurements, which means that the variation in impedance due to the coating is insignificant to the change in impedance with hydrogen.

7. Portable Electromagnetic Probe Development

Impedance results due hydrogen, temperature, and microstructure have proven successful. The next step in having an impedance analysis for in-field use requires the use of equipment that is portable and robust. Figure 38 shows an LCR precision meter from Agilent technologies with a frequency ranging from 10 Hz up to 1 MHz. The frequency range is very important because to guarantee depth of measurement, the lower frequency is better especially when conducting experiments through coatings. This LCR meter can be set-up with a laptop containing all of

the calibration curves and then it can be utilized in the field. The largest difference between this LCR Precision meter in Figure 38 and the Hewlett Packard 4275A Multi-Frequency LCR Meter utilized in the experiments for this research is that the Hewlett Packard unit has the capability of performing frequency sweeps unlike the Agilent unit. The Agilent unit on the other hand operates at lower frequencies allowing for measurements to be performed with more stand-off distance and larger pipelines.



Figure 38: Agilent technologies E4980 LCR Precision meter.

8. Application of In-field Impedance Analyzer

The results presented in Sections 5 and 6 demonstrate the success of low frequency impedance analysis for use as a hydrogen sensor for coated pipelines, however the details on how this equipment will work in the field has not been described. Figure 37 indicates that the impedance analysis can be utilized to measure additional variables. The additional variables make up the y-intercept of the data and the changes in hydrogen content are a function of the slope of the curve in Figure 37. To actually separate out the variables is difficult because impedance analysis would give one impedance value, which includes all of the variables such as: hydrogen, temperature, and microstructure.

Before low frequency measurements are performed to determine hydrogen content in coated pipelines, calibration curves and standards must be developed which include measurements being performed on many microstructures at various temperatures and hydrogen contents. Figure 39 is a schematic illustration of a calibration map for five different samples labeled A, B, C, D, and E, each having a specific microstructure, temperature, and hydrogen content. To utilize low frequency impedance measurements in the field requires at least five impedance measurements to be performed within a certain distance of one another e.g. 24 inches of pipe being exposed or through a coating. Each of these

five impedance measurements made on the pipeline are important because the microstructure and the temperature are going to be the same at each of these points of measurement, so that the only variable would be changing hydrogen content. Having a specific microstructure and temperature in the pipeline will set the y-intercept of the plot shown in Figure 39 then the variation in hydrogen content will fall on the same line having the same slope. For example, five measurements can be made and these five measurements will create line such as Line A on Figure 39. All prior measurements will lie on this line, so each impedance value will correspond to the hydrogen content value for Line A.

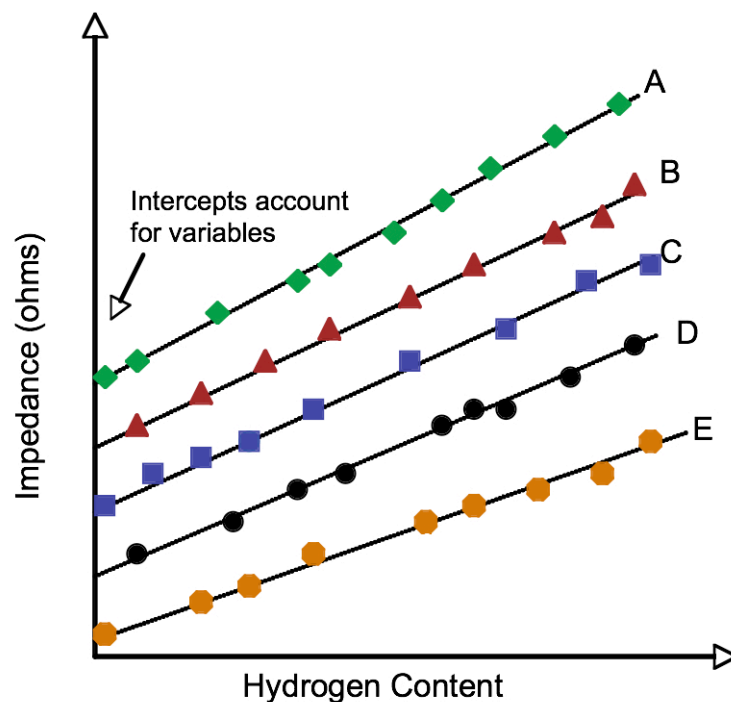


Figure 39: Schematic plot of impedance as a function of hydrogen content illustrating a calibration map for various materials A, B, C, D, and E. The y-intercept accounts for variables and the slope of each line changes with variable hydrogen contents.

9. Conclusions

The results for electromagnetic analysis of coated X80 steel linepipe cylindrical specimens show that there is another non-destructive technique available for hydrogen content assessment. This electromagnetic technique is especially unique due to its ability to be a non-contact hydrogen sensor. The results also indicate that the same

induced current impedance measurements can also be utilized to account for all additional variables in the pipeline.

10. Future Work and Recommendation

This work has shown that hydrogen contents can be measured under very specific conditions including type of steel, temperature, and microstructure. The next step in this work is to begin creating calibration curves for various linepipe steels. After calibration curves have been made for linepipe steels, then low frequency impedance experiments will be performed for hydrogen content measurements in steel weldments.

11. References

American Welding Society, "Standard Methods for Determination of Diffusible Hydrogen Content", ANSI/AWS, A4.3-93, AWS, Miami, FL, (1993).

Beachem, C.D., Hydrogen Damage, American Society for Metals, Metals Park, Ohio (1977) pp. ix-xxiii.

Beachem, C.D., "A New Model for Hydrogen Assisted-Cracking", *Metallurgical Transactions*, 3(2), pp. 437.

Bernstein, I.M., "The Effect of Hydrogen on the Deformation of Steel", *Scripta Metallurgica*, Vol. 8, (1974), pp. 343-349.

Birnbaum, H.K., "Hydrogen Effects on Deformation – Relation Between Dislocation Behaviour and the Macroscopic Stress-Strain Behaviour", *Script Metallurgica*, Vol. 31, (1994), pp. 149-153.

Blitz, J., Electrical and Magnetic Methods of Nondestructive Testing, IOP Publishing Ltd., New York, New York, (1991), pp. 35-38, 79-85, 89-166.

Bond, G.M., Robertson, I.M., and Birnbaum, H.K., "On the Determination of the Hydrogen Fugacity in an Environmental Cell TEM Facility", *Scripta Metallurgica*, Vol. 20 (1986), pp. 653-658.

Bond, G.M., Robertson, I.M., and Birnbaum, H.K., "The Influence Hydrogen on Deformation and Fracture Processes in High Strength Aluminum Alloys", *Acta Metallurgica*, Vol. 35, (1987) pp. 2289-2296.

Bray, D.E. and Stanley, R.K., Non-Destructive Evaluation: A Tool in Design, Manufacturing, and Service, Rev. Ed., CRC Press, Inc., Boca Raton, FL,(1997).

Chopra, H.D., Hicho, G.E., and Swartzendruber, L.J., “Review of the Jumpsum Based Nondestructive Testing Method for Evaluating Mechanical Properties of Ferromagnetic Materials”, *Materials Evaluation*, October, (2001), pp. 1215 – 1222.

Darken, L.S. and Smith, R.P., “The Behavior of Hydrogen in Steel During and After Immersion in Mild Acid,” *Corrosion*, Vol. 5, (1949), pp. 1-16.

Fukai, Y., The Metal Hydrogen System: Basic Bulk Properties, Springer Series in Material Science, New York, (1993).

Griffith, J.C., Krotke, R.G., and Everett, B.L., “Large Diameter Piping Examination Using Eddy-Current”, *Materials Performance*, January (1997), pp. 58-63.

Griffiths, D.J., Introduction to Electrodynamics, 3rd Ed., Prentice Hall, Upper Saddle River, New Jersey, (1999), pp. 203-342.

Kittel, C., Introduction to Solid State Physics, 7th Ed., John Wiley & Sons, New York, Chapter 6: Free Electron Fermi Gas and Chapter 7: Energy Bands, (1996), pp. 143-196.

Klümper-Westkamp, H., Mayr, P., Reimche, W., Felste, K., Bernard, M., Bach, F.W., “Non-destructive Determination of the Carbon Content in Iron Foils- A Quality Assurance of the Gas Carburizing Process”, *Intl. Symposium NDT-CE*, (2003).

Klümper-Westkamp,H.; Mayr, P.; Reimche, W.; Feiste, K.L.; Bernhard, M.; Bach, F.-W.: Bestimmung des Kohlenstoffgehaltes in Aufkohlungsfolien.*HTM* 57 (5), (2002), pp. 364-372.

Lynch, S.P., “Hydrogen Embrittlement and Liquid-Metal Embrittlement in Nickel Single Crystals”, *Scripta Metallurgica*, Vo. 13, (1979), pp. 1051-1056.

Lynch, S.P., “Environmentally Assisted Cracking: Overview of Evidence for an Adsorption-Induced Localized Slip Process”, *Acta Metallurgica*, Vol. 36, (1988), pp. 2639-2661.

Lynch, S.P., “Mechanisms of Hydrogen Assisted Cracking – A Review”, *Intl. Conf. on Hydrogen Effects on Material Behavior and Corrosion Deformation Interactions*, Moran, Wyoming, September 16-21, (2001).

Mandal, K., Dufour, D., and Atherton, D.L., "Use of Magnetic Barkhausen Noise and Magnetic Flux Leakage Signals for Analysis of Defects in Pipeline Steel", IEEE Trans., Vol. 35, No. 3, May, (1999), pp. 2007-2017.

Matsumoto, T., Eastman, J., and Birnbaum, H.K., "Direct Observation of Enhanced Dislocation Mobility Due to Hydrogen", Scripta Metallurgica, Vol. 15, (1981), pp. 1033-1037.

Mott, N.F., Jones, H., "The Theory of the Properties of Metals and Alloys", Dover Publication, Inc., New York, (1958), pp 313.

Murayama, R., Nakata, Y., Wakibe, Y., Wada, H., Imagawa, Y., and Hayashi, T., "Long Distance Inspection of Pipes Using Electromagnetic Acoustic Transducer for Cylindrical Wave", Materials Vol. 270-273, (2004), pp. 612-618.

Paskin, A., Sieradzki, K., Som, D.K. and Dienes, G.J., "Dislocation Enhancement and Inhibition Induced by Films on Crack Surfaces", Acta Metallurgica, Vol. 31, (1983), pp. 1253-1265.

Peckner, D. and Bernstein, I. M., Handbook of Stainless Steels, McGraw-Hill, New York, (1977), pp 4-3.

Pepperhoff W., and Acet, M., Constitution and Magnetism of Iron and Its Alloys, Springer-Verlag, Berlin, Heidelberg (2301), pp 146-162.

Pumarega, M.I.L., Ruiz, A., Piotrkowski, R., and Ruzzante, J., "Barkhausen Noise and Magnetic Acoustic Emission in AISI 1020 Steel with Varying Microstructure, Load, and Irradiation Damage", 4th E-GLEA Global Meeting, Octo. 16-19, Taormina, Italy, (2005).

Li, Q., Liu, Z., Miao, I., and Yuan, Z., "Theoretical Analysis of the Influence of Different Microstructure on Barkhausen Noise", Roma 2000, Proceedings of the 15th WCNDT, (2000).

Quintana, M.A., "A Critical Evaluation of the Glycerin Test", Welding Journal 63(5), (1984), pp. 141s-149s.

Quintana, M.A. and Dannecker, J.R., "Diffusible Hydrogen Testing by Gas Chromatography", Hydrogen Embrittlement: Prevention and Control, ASTM STP 962, Philadelphia, PA, (1988), pp. 247-268.

Sibilia, J.P., Materials Characterization and Chemical Analysis, 2nd Ed., VCH Publishers, New York, (1996), pp 61-217.

Smith, D.P., Hydrogen in Metals, University of Chicago Press, Chicago, (1948).

Smith II, R.D., Landis, G.P., Maroef, I., Olson, D.L., and Wildeman, T.R., "The Determination of Hydrogen Distribution in High Strength Steel Weldments Part 1: Laser Ablation Methods", AWS, Welding Research Supplement, May, (2001), pp. 115-121.

Smith II, R.D., Benson, D.K., Maroef, I., Olson, D.L. and Wildeman, T.R., "The Determination of Hydrogen Distribution in High Strength Steel Weldments Part 2: Opto-Electronic Diffusible Hydrogen Sensor", AWS, Welding Research Supplement, (1997), pp. 122-126.

Smith II, R.D., Benson, D.K., Landis, G.P, Olson, D.L, and Wildeman, T.R., "Advanced Methods for Hydrogen Determination in High Strength Steel", Proc. Intl. Conf. on Joining of Advanced and Specialty Materials II, Cincinnati, OH, Nov., (1999).

Speidel, M.O. and Pedrazzoli, R.M., "Stress Corrosion Cracking of High Strength Steel", Material Performance, Vol. 31, (1992), pp. 59.

Stanley, J.K., Electrical and Magnetic Properties of Metals, American Society for Metals, Metals Park, Ohio, (1963), pp. 207-265.

Tabata, T. and Birnbaum, H.K., "Direct Observations of the Effect of Hydrogen on the Behavior of Dislocation Mobility due to Hydrogen", Vol. 17, (1983), pp. 947-950.

Tabata, T. and Birnbaum, H.K., "Direct Observations of Hydrogen Enhanced Crack Propagation in Iron", Scripta Metallurgica, Scripta Metallurgica, Vol. 18, (1984), pp. 231-236.

Thomson, R., Chuang, T.-J., and Lin, I.-H., "The Role of Surface Stress in Fracture", Acta Metallurgica, Vol. 34, (1986), pp. 1133-1143.

Troiana, A.R., "General Keynote Lecture", in Hydrogen in Metals, I.M. Bernstein and A.W. Thompson (ed.), ASM, Metals Park Ohio, (1974), pp. 3-15.

Wilkes, P., Solid State Theory in Metallurgy, Cambridge University Press, London, England, (1973), pp. 126-131, 285-293.

Williams, H.J. and Shockley, W., "A Simple Domain Structure in an Iron Crystal Showing a Direct Correlation with Magnetization", Phys. Review, 75, (1949), pp. 178-183.

Wiswall, R., "Hydrogen Storage in Metals", in Hydrogen in Metals II, Springer Verlag, Berlin, Germany, (1978), pp. 201-242.

Zemansky, M.W., Heat and Thermodynamics, 4th Ed., McGraw-Hill, Pennsylvania, (1957), pp. 298-302.

Websites:

www.leco.com

<http://www.cartage.org.lb/en/themes/Sciences/Physics/SolidStatePhysics/MagneticProperties/Squid/Configuration/Configuration.htm>

<http://www.pubs.acs.org/cen/80th/elements.html>